UNIVERSITA DEGLI STUDI DI PARMA

Dottorato di Ricerca in Medicina Molecolare

Ciclo XXIX

Striatin-gene loss of function induces functional alterations in a haploid stem cell mouse model for cardiomyogenic differentiation

Coordinatore:
Chiar.mo Prof. Luciano Polonelli

Tutor Interno:
Chiar.mo Prof.ssa Donatella Stilli

Tutor Esterno - EURAC Research:
Dott.ssa Alessandra Rossini

Dottorando: Gennaccaro Laura

"*Luck is what happens when preparation meets opportunity*."

— Seneca

I dati e i metodi di ricerca originali descritti in questo elaborato sono coperti da embargo fino al 1 giugno 2019 in quanto facenti parte di un progetto di ricerca/studio più ampio avviato da Accademia Europea di Bolzano, conformemente a quanto previsto dalle linee guida fornite dall´Università di Parma.

Data and research methods described in this thesis are part of a wider research project of European Academy of Bolzano and are protected by embargo until June 1st 2019, in accordance with the guidelines provided by the University of Parma.

L´uso delle illustrazioni e delle tabelle contenute nelle sezioni Introduzione e Materiali e Metodi di questo elaborato è stato debitamente richiesto e autorizzato dall´avente titolo, riportato in citazione e referenza.

Permissions to use figures and tables shown in the Introduction and Materials and Methods sections of this thesis have been required and obtained from the rights holder of the material.

Index

Tables

Figures

List of abbreviations

Action Potential	***AP***
Action Potential Amplitude	***APA***
Action Potential Duration	***APD***
ATPase sarcoplasmic reticulum Ca^{2+} transporting2	***ATP2A2 or SERCA2A***
Intracellular calcium	***Ca_i***
Calcium Channel 1C/G/H Subunit	***CACNA1C/G/H***
Calmodulin	***CaM***
Cardiomyocytes	***CMs***
Caveolin 1	***Cav-1***
B-catenin	***CTNNB1***
Embryoid Bodies	***EBs***
Embryonic Stem Cells	***ESC***
Embryonic Stem Cell Medium	***ESCM***
Fetal Bovine Serum	***FBS***
Hyperpolarization-activated cyclic nucleotide–gated channel	***HCN***
Inter-event-interval	***IEI***
Na^+-Ca^{2+} exchange current	***I_{NCX}***
Leukemia Inhibitory Factor	***LIF***
Potassium voltage-gated channel subfamily J	***KCNJ***
Maximum Diastolic Potential	***MDP***
Mouse embryonic fibroblast	***MEF***
Mouse embryonic stem cells	***mESCs***
NK2 transcription factor related, Locus-5	***Nkx2.5***
Phosphate Buffered Saline	***PBS***
Real Time-Polymerase Chain Reaction	***RT-PCR***

Ryanodine receptor channel	***RyR***
Sodium Channel protein type 5 subunit α	***SCN5A***
Striatin interacting phosphatase and kinase	***STRIPAK***
Sarcoplasmic reticulum	***SR***
Striatin	***Strn***
Transmembrane potential	***TMP***
Tryptophan-aspartate	***WD***
Wild Type	***WT***

Abstract

Background Striatin (Strn) is a ubiquitous Ca^{2+}-dependent scaffolding protein that in cardiomyocytes (CMs) co-localizes at the intercalated disc region with desmosomal proteins. Recent studies demonstrated that a deletion in the 3' untranslated region of the STRN gene was associated with arrhythmogenic right ventricular cardiomyopathy and dilated cardiomyopathy in dogs. Moreover, the Striatin gene was also recently associated with cardiac abnormalities in Drosophila melanogaster.

Mouse embryonic stem cells (mESCs) with a haploid chromosomal set have recently been suggested as a good tool for genetic screens. They retain the capacity to differentiate into the three germ layers *in vitro* and, possessing just one copy of each gene, they facilitate the generation of loss-of-function mutants that represent a powerful tool to investigate the role of new target genes. Preliminary evidence obtained in our laboratory indicates that Strn knock out could impact the electrophysiological properties of haploid mESC-derived cardiomyocytes (CMs).

Objectives This thesis tries to elucidate how the Strn cellular depletion affects the functional characteristics of haploid mESC-derived CMs. To this aim, a Strn-mutant line of haploid mESC line (namely 377C05) generated by gene trapping by J. Penninger and co-workers was used. This mutant and the corresponding wild-type (WT) line were used as cell models for this project.

Methods The differentiation protocol based on the hanging drop technique was modified to optimize the appearance of beating embryoid bodies (EBs) from haploid mESCs. The cardiomyogenic differentiation process was evaluated at the functional, morphological and molecular level in the Strn-mutants and compared to WTs. Specifically, the contractility properties of the beating areas were assessed by video tracking analysis, spontaneous action potentials (APs) were recorded by current clamp, and intracellular calcium concentration was simultaneously monitored in Fluo-4 loaded EBs. Structural changes of haploid mESC-derived CMs immunostained for Troponin-T were evaluated by confocal microscope, while changes in the expression of pluripotency genes, cardiac differentiation markers, Strn interacting proteins and ion channels were estimated by quantitative Real time-PCR. All the data were analyzed using non-parametric statistical tests.

Results At day 12 of differentiation, we found a significant decrease in the number and the dimension of beating areas in Strn-mutant as compared with WT, together with a significant lower frequency of contraction and a dysregulated (arrhythmic) contraction behavior. However, when the frequency of APs was evaluated, it appeared higher in Strn-mutant. Furthermore, the AP duration was decreased, as well as the duration of the diastolic depolarization phase, possibly suggesting an alteration in the

EC-coupling process. Thus, the calcium-induced calcium release process was investigated by simultaneous recordings of spontaneous APs and their induced calcium transients. Intriguingly, no differences were observed: in fact, every AP was aligned with a calcium spike. However, when we evaluated the delay between each AP peak and its correspondent calcium peak, we observed a trend of increased delay in the mutants versus WTs. In addition, the amount of Ca^{2+} released after spontaneous APs in the mutant was about twice lower than in the WTs.

Further, the sarcomere structure analysis showed that 49% of CMs, obtained from Strn-mutant, presented sarcomeres with an absence of the striated configuration for Troponin-T.

When gene expression was investigated, we found a significant upregulation of β-catenin and HCN4 expression in Strn-mutants.

Conclusions Here we provide evidence that Strn-mutants are characterized by: (i) alteration in APs frequency and action potential duration, (ii) reduced contraction frequency and beating area dimension, (iii) delayed Ca^{2+} release (iv) reduced amplitude of Ca^{2+} transients and (v) structural alteration of the sarcomere.

Overall, these results indicate that Strn has a strong impact on CMs function, possibly representing a new molecular target for the identification of new causes and therapies of cardiovascular disease.

Riassunto

STUDIO DELL'EFFETTO DELLA MUTAZIONE DI STRIATINA SUL DIFFERENZIAMENTO CARDIACO MEDIANTE L'UTILIZZO DI UN MODELLO DI CELLULE STAMINALI MURINE APLOIDI

Introduzione: Striatina (Strn) è una proteina scaffold, in grado cioè di mediare l'interazione fra proteine diverse permettendone la corretta funzione. È una proteina ubiquitaria calcio-dipendente che, nei cardiomiociti (CMs) si localizza nei dischi intercalari con le proteine desmosomiali. Studi recenti hanno dimostrato come una delezione nella regione 3' non tradotta del gene di STRN nei cani è associata sia alla cardiomiopatia aritmogena sia alla cardiomiopatia dilatativa. Infine, il gene codificante per Striatina è stato recentemente associato ad alterazioni cardiache in Drosophila Melanogaster.

Le cellule staminali embrionali murine (mESCs) con un set cromosomico aploide sono state recentemente considerate come un buon modello per screening genetici. Esse mantengono la capacità di differenziare *in vitro* nei tre foglietti embrionali e, possedendo solo una copia di ogni gene, facilitano la creazione di mutanti con perdita di funzione (knock-out) che rappresentano un potente strumento per studiare il ruolo di nuovi geni bersaglio.

Evidenze preliminari ottenute nel nostro laboratorio indicano come la rimozione dell'espressione di Striatina possa influenzare le proprietà elettrofisiologiche dei CMs ottenuti da mESCs aploidi.

Obiettivi: Scopo del presente lavoro è stato chiarire come la mancanza di Strn abbia conseguenze sulle caratteristiche funzionali dei CMs ottenuti dalle mESCs aploidi. A questo scopo, è stata utilizzata una linea di cellule mESCs aploidi mutanti per Strn, chiamata 377C05 e prodotta da J. Penninger e collaboratori tramite 'gene trapping'. Tale linea mutante e la rispettiva linea controllo (WT) sono state utilizzate come un modello cellulare per questo progetto.

Metodi: Il classico protocollo di differenziamento basato sulla "goccia pendente" è stato modificato per ottimizzare la comparsa di corpi embrioidi (EBs) battenti dalle mESCs aploidi. Il processo di differenziamento cardiomiogenico è stato valutato a livello funzionale, morfologico e molecolare nel mutante di Strn e confrontato con il WT.

In particolare, le capacità contrattili delle aree battenti sono state valutate mediante analisi di video tracking, i potenziali di azione (APs) sono stati registrati tramite current-clamp, e la concentrazione di calcio intracellulare è stata contemporaneamente registrata grazie all'utilizzo del colorante calcio dipendente Fluo-4.

Infine, i cambiamenti a livello dell'organizzazione sarcomerica sono stati valutati mediante analisi confocale sui CMs ottenuti dalle mESCs aploidi utilizzando un anticorpo per la Troponina-T, mentre variazioni nell´espressione dei geni di pluripotenza, dei marcatori della differenziazione cardiaca, dei canali ionici e di alcune proteine che interagiscono con Strn sono stati saggiati mediante Real time-PCR quantitativa. Tutti i dati sono stati esaminati usando test statistici non parametrici.

Risultati:

Al giorno 12 di differenziazione, nel mutante per Strn sono state riscontrate differenze significative rispetto al WT nel numero e nelle dimensioni delle aree battenti, insieme ad una frequenza di contrazione più bassa e un andamento irregolare della contrazione (aritmia). Tuttavia, la frequenza degli APs spontanei risultava più alta nei mutanti. Inoltre, la durata degli APs era minore, così come la durata della fase di depolarizzazione diastolica, suggerendo un´alterazione a livello del processo di eccito-contrazione. Si è pertanto deciso di indagare la dinamica del calcio (Calcium-induced calcium release) intracellulare attraverso registrazioni simultanee dei APs spontanei e dei transienti di calcio da essi indotti.

Curiosamente, nessuna differenza è stata osservata: infatti ogni APs era allineato con un picco di calcio. Sebbene quando si è valutato il tempo tra ogni picco di APs e il corrispondente picco di calcio, è stato osservato un trend di aumento del ritardo nel rilascio di calcio nel mutante rispetto al controllo. Inoltre, la quantità di Ca^{2+} rilasciato dopo ogni AP spontaneo, nel mutante era circa due volte minore rispetto al WT.

Infine, l'analisi della struttura sarcomerica ha mostrato che il 49% di CMs, ottenuto dal mutante per Strn, non presentava nei sarcomeri la tipica configurazione striata della troponina-T.

Infine nella linea mutante, si è riscontrato un aumento statisticamente significativo per l´espressione dell´mRNA della β-catenina e del canale HCN4.

Conclusioni: I nostri dati mostrano che i mutanti per Strn sono caratterizzati da: (i) alterazione della frequenza e nella durata degli APs, (ii) riduzione nella frequenza di contrazione e nella dimensione delle aree battenti, (iii) ritardo del picco del transiente di calcio rispetto al picco dell'AP corrispondente, (iv), ridotta ampiezza dei transienti di Ca^{2+} rilasciato dopo ogni AP spontaneo e (v) alterazione strutturali dei sarcomeri.

Nel complesso, questi risultati indicano che Strn ha un forte impatto sulla funzione dei cardiomiociti, suggerendo Strn come un nuovo possibile bersaglio molecolare nell'individuazione di cause e possibili cure delle patologie cardiovascolari.

Introduction

1. *The basis of cardiomyocyte (CMs) physiology*

The heart is the muscle that pumps blood throughout the whole body for the person's lifetime. The contraction force is generated by cardiac muscle cells, or cardiomyocytes (CMs). Atrial and ventricular CMs contract following an electrical stimulus (De Souza et al., 2013). In the healthy heart, the electrical impulses originate as spontaneous action potentials (APs) in the sinoatrial node (SAN), spread rapidly through the atrial CMs, and join the atrioventricular node (AVN). The impulse is then conducted by the His-Purkinje system through the ventricles (Gourdie et al., 2003).

Four properties of cardiac tissue enable the initiation and conduction of APs and myocardial contractility (Bers, 2002):

- Automaticity, is the ability of specialized tissue cells in the SA node, part of the atria, and AVN to spontaneously initiate impulses
- Excitability, is the ability of the myocardial tissue to be depolarized by stimulus
- Conductivity, is the transmission of APs from one CM to another
- Contractility, is the ability of the myocardial cells to shorten.

1.1 The cardiac Action Potential and impulse conduction

Cardiac action potentials are generated by the movement of ions through the transmembrane ion channels in the cardiac cells (Nerbonne and Kass, 2005).

Figure 1 illustrates the 5 phases of the normal cardiac (ventricular) action potential:

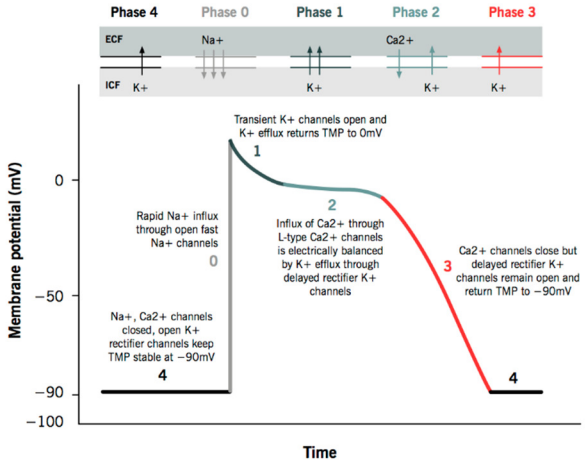

Fig. 1 Action Potential of cardiac muscles Used with permission from Grigoriy Ikonnikov, Eric Wong, and Sultan Chaudhry. McMaster Pathophysiology Review, www.pathophys.org

- *Phase 0* is the phase of rapid depolarization. An action potential triggered in a neighboring cardiomyocyte or pacemaker cell causes the transmembrane potential (TMP) to rise above −90 mV. The Fast Na^+ channels start to open one by one and Na^+ leaks into the cell, so the TMP approaches −70mV, the threshold potential in cardiomyocytes, i.e. the point at which enough fast Na^+ channels have opened to generate a self-sustaining inward Na^+ current. Now the large Na^+ current rapidly depolarizes the TMP to 0 mV and slightly above 0 mV for a transient period of time called the overshoot; fast Na^+ channels close (recall that fast Na^+ channels are time-dependent). Finally the L-type ("long-opening") Ca^{2+} channels open when the TMP is greater than −40 mV and cause a small but steady influx of Ca^{2+} down its concentration gradient.
  This phase is central to rapid propagation of the cardiac impulse (conduction velocity, 1 m/s).
- *Phase 1* is a phase of rapid repolarization. This phase sets the potential for the next phase of the action potential. Some K^+ channels open briefly and an outward flow of K^+ returns the TMP to approximately 0 mV.
- *Phase 2*, a plateau phase, is the longest phase. L-type Ca^{2+} channels are still open and there is a small, constant inward current of Ca^{2+}. This becomes significant in the excitation-contraction coupling process described below. K^+ leaks out down its concentration gradient through delayed rectifier K^+ channels. These two countercurrents are electrically balanced, and the TMP is maintained at a plateau

just below 0 mV throughout phase 2 (in this phase also the slow Na^+ currents could play an important role)

- *Phase 3* is the phase of final repolarization that restores the membrane potential to its resting value.

  The Ca^{2+} channels are gradually inactivated, while the persistent outflow of K^+, now exceeding Ca^{2+} inflow, brings TMP back towards resting potential of −90 mV to prepare the cell for a new cycle of depolarization.
  Normal transmembrane ionic concentration gradients are restored by returning Na^+ and Ca^{2+} ions to the extracellular environment, and K^+ ions to the cell interior. The pumps involved include the sarcolemmal Na^+-Ca^{2+} exchanger, Ca^{2+}-ATPase and Na^+-K^+-ATPase.
- *Phase 4:* The resting potential in a cardiomyocyte is restored (at −90 mV) due to a constant outward leak of K^+ through inward rectifier channels and Na^+ and Ca^{2+} channels are closed at resting of the TMP.

From the beginning of phase 0 until part way through phase 3 when the membrane potential reaches -60mV, each cell is in an absolute refractory period, also known as the effective refractory period, during which it is impossible to evoke another action potential. This is immediately followed until the end of phase 3 by a relative refractory period, during which a stronger-than-usual stimulus is required (Purves and Sakmann, 1974). The refractory period of cardiac cells is an important control which is used by cells in order to control the onset of another wave; in fact, this process inhibits arrhythmias, preventing that whenever a cell depolarizes, which are those near are enabled.
In plus the refractory period helps coordinate muscle contraction forcing the depolarization to spread outward, respect where generated.(Taglietti and Casella, 2004)

1.2 E-C coupling: The calcium-induced calcium release theory

The functions of the electrical system of the heart are not only initiation and rate of the heart beat, but its coordinated transmission to the entire heart resulting in maximum mechanical efficiency. Excitation-contraction coupling represents the process by which an electrical action potential leads to contraction of cardiac muscle cells. This is achieved by converting a chemical signal into mechanical energy via the action of contractile proteins (Bers, 2002). Each myocyte is made up of many myofibrils which are aligned along the long axis of the cell. In turn, each myofibril is made up of sarcomeres which are joined in series. The sarcomeres contain interdigitating myofilaments made

up of contractile proteins. The cell surface is covered with sarcolemma, which forms invaginations between each of the sarcomeres. This is the source of calcium, which is released when the membrane is depolarized (Woodcock and Matkovich, 2005). The contractile fibres contain four proteins. Two proteins form filaments which overlap; the thicker filament is myosin, the thinner, actin. Two regulatory proteins, troponin and tropomyosin, are involved in the formation of cross-bridges between the two filaments (Okada et al., 2008). When the cell is stimulated by an excitatory impulse, a complex movement of ions, particularly the release of calcium stored in the sarcoplasmic reticulum (SR), results in an increase in the overlap of the myofilaments and a consequent reduction in the length of the filament and cell (i.e. contraction).

Specifically, when an action potential reaches a contractile cell, it spreads along the sarcolemma and T tubules, at the level of which determines the opening of voltage-dependent channels for Ca^{2+} present in the cell membrane. Through these channels, calcium enters the cell and promotes the opening of the ryanodine receptor-channels (RyR) in the endoplasmic reticulum (ER) (Diaz-Sylvester et al., 2011, Lanner et al., 2010). The receptors for the ryanodine are channels for Ca^{2+} and their opening triggers a process known as calcium-induced Ca^{2+}release. The Ca^{2+} accumulated in the sarcoplasmic reticulum flows into the cytosol, causing a "download" of Ca^{2+}.Calcium spreads through the cytosol to the contractile elements, where the ions bind to troponin and trigger the formation cycle of cross bridges and then the movement.

As soon as the Ca^{2+} concentration decreases, these ions are detached from troponin, actin and myosin releases the contractile filaments slide back towards their rest position. The Ca^{2+} ions are then transported into the sarcoplasmic reticulum with the help of a Ca^{2+}-ATPase and by a Na^{+}-Ca_2^{+} antiporter protein (Van Petegem, 2012)

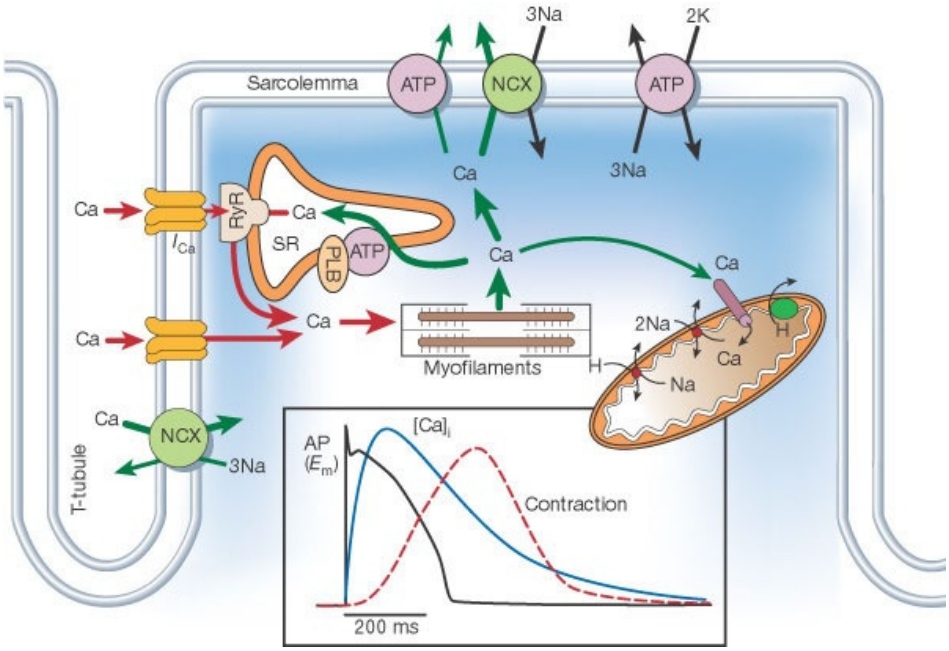

Fig. 2 Scheme of cardiac excitation-contraction-coupling events in a ventricular myocyte. (Bers ,D.M., 2002)

1.3 Autorhythmicity

Autorhytmicity or automacity are defined by heart physiology, as the ability to spontaneously depolarize of specialized cardiac cells that generate periodical electrical oscillations (Taglietti and Casella, 2004). Even if the signaling cascade initiating the pacemaker cycle in automatic cells is still not entirely understood, ion channels and intracellular Ca^{2+} signaling seem to have an important role in setting the pacemaker mechanism.

The "voltage clock" mechanism

Silvio Weidmann started applying the Hodgkin–Huxley formalism of membrane excitation to interpret the cardiac electrical activity, including the pacemaker depolarization, in a pioneering study about 50 years ago (Noble, 1979). The main concept was that the generation of the cardiac pacemaker AP and also the control of the spontaneous depolarization between APs and thus the determination of when the next AP would occur are dependent by the voltage and time-dependent gating of different surface membrane channels. Surface membrane ion channels work together regulating the rate and rhythm of spontaneous AP firing, otherwise known as normal automaticity, as a clock. Because the

membrane ionic channels open and close according to the membrane potential, this process is referred to as membrane voltage clock (Joung et al., 2009).

The "Funny" Current, If

Although different ionic conductances could be related with the automaticity behavior, based on a wealth of experimental evidence, *If* is today considered as the most important ion channel involved in the rate regulation of cardiac pacemaker cells, and is sometimes referred to as "the pacemaker channel." As it was clear since the current was first described in 1979 in the SA node (Brown et al. 1979b), the diastolic depolarization phase of the action potential, which is responsible for normal spontaneous activity is generated by funny channels, characterized by specific properties. It activates upon hyperpolarization, one of the unusual features which at the time of its discovery made the current deserve the attribute "funny", at a threshold of about −40/−50 mV, and is fully activated at about −100mV. In its range of activation, which quite properly comprises the voltage range of diastolic depolarization, the current is inward, its reversal occurring at about −10/−20 mV. This is due to the mixed Na^+/K^+ permeability of f-channels (DiFrancesco, 1993).

Another unusual feature of If is its dual activation by voltage and by cyclic nucleotides. Cyclic adenosine monophosphate (cAMP) molecules bind directly to if-channels and increase their open probability (DiFrancesco and Mangoni, 1994, DiFrancesco and Tortora, 1991). cAMP dependence is a particularly relevant physiological property, since it underlies the *If*-dependent autonomic regulation of heart rate (Brown et al., 1979, DiFrancesco, 1993, DiFrancesco et al., 1989).

In the late 1990s, almost two decades after the first description of *If*, a family of genes encoding the molecular correlates of pacemaker channels was finally sequenced and cloned (Ishii et al., 2001, Ludwig et al., 1999, Seifert et al., 1999, Vaccari et al., 1999). These genes and the corresponding protein products were named hyperpolarization-activated, cyclic nucleotide-gated (HCN) channels; four isoforms are known in mammals (HCN1–4). One of the four HCN isoforms (i.e. .HCN4) is the most highly expressed in the SAN (Shi et al., 1999, Liu et al., 2007).

The "calcium clock" mechanism

The spontaneous release of Ca^{2+} from the sarcoplasmic reticulum was recently suggested as an additional mechanism of sinus rhythm generation also known as the Ca^{2+} clock. The observation that application of ryanodine slowed subsidiary pacemakers in cat right atrium led to identification of

intracellular calcium (Ca_i) cycling as heart rhythm generator (Rubenstein and Lipsius, 1989). Electrogenic Na^+-Ca^{2+} exchanger current (I_{NCX}) were also showed to be involved in pacemaker activity by different works, and it was underlined that an increase in Ca^{2+} release followed by activation of I_{NCX} could play a role in the positive chronotropic effect of β-adrenergic stimulation in latent pacemaker cells (Huser et al., 2000, Ju and Allen, 1998, Li et al., 1997). It was proposed by Lakatta et al. that the spontaneous rhythmic SR Ca^{2+} release in SAN cells, exhibited as Ca^{2+} sparks, works as the "Ca^{2+} clock". The elevated Ca^{2+} causes diastolic depolarization via I_{NCX} activation, which coordinately regulates sinus rate along with the voltage clock (Maltsev et al., 2006, Vinogradova et al., 2002, Vinogradova et al., 2006). The mechanism of automaticity, as the idea of Ca^{2+} clock suggests, is the same as that of delayed afterdepolarization, which occurs when there is SR Ca^{2+} overload. This underlines the natural existence of the SAN in a state of calcium overload.

Abnormalities in automaticity

A number of ion channels and transporters are required to have a finely orchestrated activity to guarantee normal heart rhythm and an orderly propagation of electrical impulses throughout the myocardium. Severe consequences derive from the disruption of either, resulting in potentially lethal heart rhythm disturbances. Primary electrical diseases including long-QT syndrome, short-QT syndrome, Brugada syndrome, and catecholaminergic polymorphic ventricular tachycardia have been

associated with mutations in a variety of ion channel subunit genes that promote arrhythmogenesis (Table 1) (Shah et al., 2005).

Primary Electric Diseases Producing Ventricular Arrhythmias

	Chromosome	Gene	Protein	Frequency	SCD Incidence	Inheritance Pattern LQTS
LQTS						
LQT1	11p15	*KCNQ1*	KvLQT1 (I_{Ks})	~50%	0.30%/y	AD, AR
LQT2	7q35	*KCNH2*	hERG (I_{Kr})	30–40%	0.60%/y	AD
LQT3	3p21	*SCN5A*	Na channel	5–10%	0.56%/y	AD
LQT4	4q25	*ANK2*	Ankyrin B	Rare		AD
LQT5	21q22	*KCNE1*	minK (I_{Ks})	Rare		AD/AR
LQT6	21q22	*KCNE2*	MiRP1 (I_{Kr})	Rare		AD
LQT7	17	*KCNJ2*	IK1	Rare		AD
SQTS						
SQTS	7	*KCNH2*	hERG (I_{Kr})	Rare		AD
SQTS	11	*KCNQ1*	KvLQT1 (I_{Ks})	Rare		AD
Idiopathic VF (Brugada syndrome)	3	*SCN5A* (>30)	Na channel			AD
CPVT						
CPVT1	1q42–43	*RYR2*	Cardiac ryanodine receptor			AD
CPVT2	1p11-p13.3	*CASQ2*	Calsequestrin			AR
CPVT3?	?	?	?			AD

AD indicates autosomal dominant; AR, autosomal recessive.

Table 1 Primary electrical diseases (Shah et al., 2005)

In a review by Verkerk and Wilders (Verkerk and Wilders, 2015) 22 mutations or variants in HCN4 associated with clinically established or potential sinus node dysfunction have been reported. However, since *If* variants reported in the literature in single patients without a clear-cut association between genotype and phenotype have been discarded, the number of sinus node dysfunction-linked mutations is reduced to 13 according to DiFrancesco (DiFrancesco, 2015).
In most cases, the dysfunctional HCN channels primarily caused bradyarrhythmias, but additional rhythm disturbances such as atrioventricular block, impaired chronotropic response, sinus pauses, tachy–brady syndrome were also observed (Baruscotti et al., 2016).

2. *Striatin: Structure and function*

In 1996 Castest and colleagues cloned a cDNA encoding a novel protein with a molecular mass of 86 KDa composed of 780 amino acids, Striatin. (Castets et al., 1996).
This protein was the first protein known to bind Calmodulin (CaM) in a calcium-dependent manner and presenting, in the carboxy-terminal part, a repeated sequence of Tryptophan- Aspartic Acid (WD) (Castets et al., 1996). The authors showed that Striatin is present in the central nervous system and

that is particularly abundant in the dorsal part of striatum (hence its name), but the role of this protein remained unknown.

In 2000, again the group of Ariane Monneron, characterized another two proteins "with Striatin identical protein-protein interaction domains and the same overall domain structure"; thus, the multigenic Striatin family was described for the first time (Castets et al., 2000).

All the three proteins belonging to the family, namely Striatin, Zinedin and SG2NA (Hwang and Pallas, 2014) are characterized by four protein-protein interaction domains: a caveolin-binding domain (Cav) necessary for localization, a coiled-coiled (C-C) domain, which allows the oligomerization, a Ca^{2+}-calmodulin-binding domain (CaM) that has been hypothesized to be the sensor responding to intracellular Ca^{2+} variation, and a Tryptophan- Aspartic Acid (WD) repeat domain important for organizing the large signaling complex. (Castets et al., 1996, Castets et al., 2000, Gaillard et al., 2001).

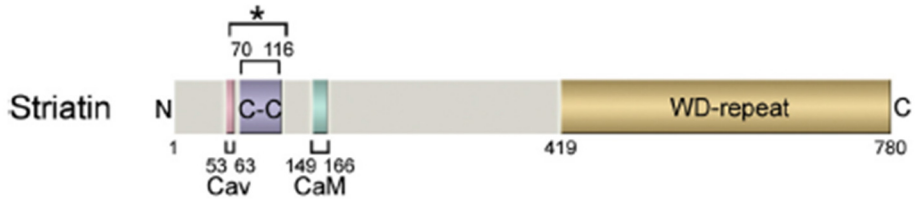

Fig. 3 Domain structure of Striatin (Hwang and Pallas, 2014).

Although originally discovered in brain tissue, Striatin has been detected in cells of other tissues and organs like cardiac intercalated disk (Franke et al., 2015, Oxford et al., 2014), and corneal epithelium (Stern et al., 2015). This indicates that the biological functions of Striatin are more widespread and not only limited to neuronal cells. Accordingly, in the last decades different theories about the function of Striatin and other members of its family were elaborated, depending on the identification and study of their associated proteins (Baillat et al., 2001, Castets et al., 2000, Goudreault et al., 2009, Moreno et al., 2001, Moreno et al., 2000). Indeed, it is known in the literature that both in prokaryotic and eukaryotic cells the Striatin family- associated proteins form a signaling complex named Striatin Interacting Phosphatase and Kinase (STRIPAK). In this complex, Striatin always interacts at least with the serin/threonine phosphatase 2a (PP2A) and with members of the germinal center kinase III (GCKIII) family (Goudreault et al., 2009).

This complex, in turn, can be associated with numerous others proteins involved in multiple signaling pathways and functions in cellular regulation. For example when the STRIPAK complex interacting with Cav-1 performs a role in caveolae- dependent endocytosis, or when the Cerebral Cavernous malformation 3 (CCM-3) protein binds the STRIPAK complex and this new complex is localized in the apical membrane, promoting Golgi stability and endocytic recycling (Lant et al., 2015)

Thus, Striatin does not have a fixed distribution pattern in the cell, and can be located at the membrane or in the cytoplasm; in addition, its localization depends on Ca^{2+} concentration (Bartoli et al., 1998, Hwang and Pallas, 2014)

3. *Evidence for Striatin as a player in cardiovascular disease*

Recently, a possible role of the STRIPAK complexes in the heart has been reported (Hwang and Pallas, 2014).
The STRIPAK associated protein SLMAP is a membrane-anchoring protein that appears to be specific for cardiac muscle. More specifically, the multicomplex is located in the T-tubules, sarcoplasmic reticulum or sarcolemma according to binding to different isoforms of SLAMP.
Guzzo and colleagues demonstrated that the STRIPAK-SLMAP complex interacts with the myofibrils, regulating the structural arrangement of the E-C coupling apparatus. (Guzzo et al., 2005)

Moreover, mutations in the Striatin gene are connected with cardiac diseases. In 2010 Sotoodehnia and colleagues, conducting a meta-analysis in European individuals from 14 genome wide association study (GWAS), demonstrated the Striatin gene as a common variant associated with the regulation of ventricular conduction and QRS interval length (Sotoodehnia et al., 2010) The QRS interval represents the electrical stimulation along the conductive tissue that corresponds to the depolarization of the right and left ventricles of the heart, and a prolonged QRS interval is associated with a common electrocardiographic abnormality associated with sudden cardiac death.

Again in 2010, Meurs and colleagues showed a reduction in Striatin mRNA levels in a canine model of arrhythmogenic right ventricular cardiomyopathy (ARVC), depending on a deletion of eight base pairs in the 3´untranslated region of the gene. Additionally, they demonstrated that Striatin protein

was localized, in the healthy dog, in the intercalated disks linked to desmosomal proteins (plakophilin 2, plakoglobin and desmoplakin) (Meurs et al., 2010).

Three years later, Meurs and colleagues, associated the same Striatin deletion with a dilated cardiomyopathy (DCM) in boxer dogs, in particularly with the homozygous genotype that presents dysfunction, dilatation and ventricular tachyarrhythmias in approximately 75% of the cases (Meurs et al., 2013).

Finally, in 2014 Oxford and colleagues demonstrated that normally ß-catenin and Strn are co-localized in the cell membrane of cardiomyocytes, at the level of cardiac intercalated disk, while a delocalization of both proteins was present in the endoplasmic reticulum in the ARVC-Boxer dogs with an increase of 50% in ß catenin protein amount (Oxford et al., 2014).

They hypothesized that a Wnt pathway dysfunction is involved in the development of ARVC promoting the progression of fibro-fatty infiltration in heart tissue (Garcia-Gras et al., 2006) by the incorrect positioning of β-catenin which is a modulator of the Wnt canonical pathway. Specifically, the accumulation of βcatenin and Striatin in the endoplasmic reticulum compromised transport to the membrane, reducing the number of adherens junctions; at the same time, the lack of translocation of βcatenin into the nucleus reduces its function as transcription factor, inhibiting the cellular pathways involved in differentiation and proliferation (Oxford et al., 2014).

4. *Embryonic stem cells as a source of cardiomyocytes*

4.1 Definition and characteristics of embryonic stem cells (ESCs)

Embryonic stem (ES) cells are derived from the inner mass of mammalian blastocysts and are totipotent, possessing the ability to give rise to all the tissues of an adult organism including the reproductive germ cells, but not extra-embryonic tissues (Ulloa-Montoya et al., 2005). When cultured *in vitro* under appropriate conditions ES cells are capable of propagating indefinitely, while maintaining unaltered their differentiation potential (Yu and Thomson, 2008). Therefore, a high developmental potency together with a high capacity for self-renewal *in vitro* are the defining features of ES cells (Czechanski et al., 2014).

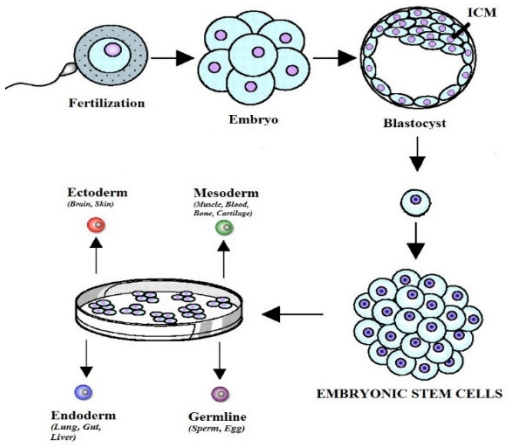

Fig. 4 Embryonic stem cells derives derived from ICM of the blastocyst: modified by (Wobus and Boheler, 2005)

4.2 In vitro cardiomyogenic differentiation of ES cells

Mouse embryonic stem cells (mESCs) are derived from pre-implantation stage embryos (Evans and Kaufman, 1981). They are characterized by the expression of pluripotency-associated factors, including Oct3/4 (Pou5f1) and Nanog (Masui et al., 2007) .

The group of Austin Smith pioneered the discovery of factors necessary to maintain mESCs in their undifferentiated state, highlighting the role of LIF/STAT3 pathway activation in promoting pluripotency (Hall et al., 2009). Several other factors, including bone morphogenic protein (BMP) (or serum) (Ying et al., 2003) and feeder layers of mitotically inactivated mouse embryonic fibroblasts (MEFs) (Bryja et al., 2006), are now known to prevent differentiation of mESCs *in vitro.*

During *in vitro* differentiation, ESCs have been shown to recapitulate many processes of early embryonic development and can develop into specialized somatic cells, including cardiomyocytes (CMs) (Xiao, 2003). mESC-derived CMs represent a powerful tool for several cardiac research areas, including developmental biology, functional genomics and pharmacological testing (Winkler et al., 2005).

Cardiac differentiation occurs spontaneously when the ES cells are removed from the feeder layer and cultivated into 3D cell aggregates, termed embryoid bodies (EBs). It is believed that the interaction occurring in the 3D structure is crucial to sustain differentiation (Bratt-Leal et al., 2009).

In fact, EBs show the typical regional expression of embryonic markers specific to different lineages of ectodermal, mesodermal, and endodermal origin (Itskovitz-Eldor et al., 2000). Many different techniques have been used to promote EBs formation. The most commonly used is the "hanging drops" technique, where a definite number of mouse ES cells (usually 400) are cultivated in hanging drops (Boheler, 2003, Wang and Yang, 2008, Wobus et al., 2002). After two days, the spheroid EBs are collected and further cultivated for five additional days in suspension. Further differentiation is achieved by transferring the EBs on coated plastic dishes where they grow in adherence (Wang and Yang, 2008). After a variable number of days, cardiomyocytes can be easily identified in the cell culture as clusters of spontaneously beating areas (Kurosawa, 2007, Ohnuki and Kurosawa, 2013, Wang and Yang, 2008). Beating areas can be then manually dissected and cells further characterized, although a fraction of fibroblasts is always present (Hashemi-Tabar, 2006).

4.3 Molecular players in cardiomyogenic differentiation

The studies on animal models have enormously increased our knowledge of the basics of cardiac differentiation mechanisms (Zaragoza et al., 2011). However, the use of *in vitro* models of cardiogenesis, such as mouse embryonic stem cells, has consistently shed more light on the molecular players governing each stage of cardiac embryogenesis (Bettiol et al., 2006) and the fact that *in vitro* cardiac differentiation is a good model for *in vivo* cardiac differentiation has been demonstrated (Rajala et al., 2011).

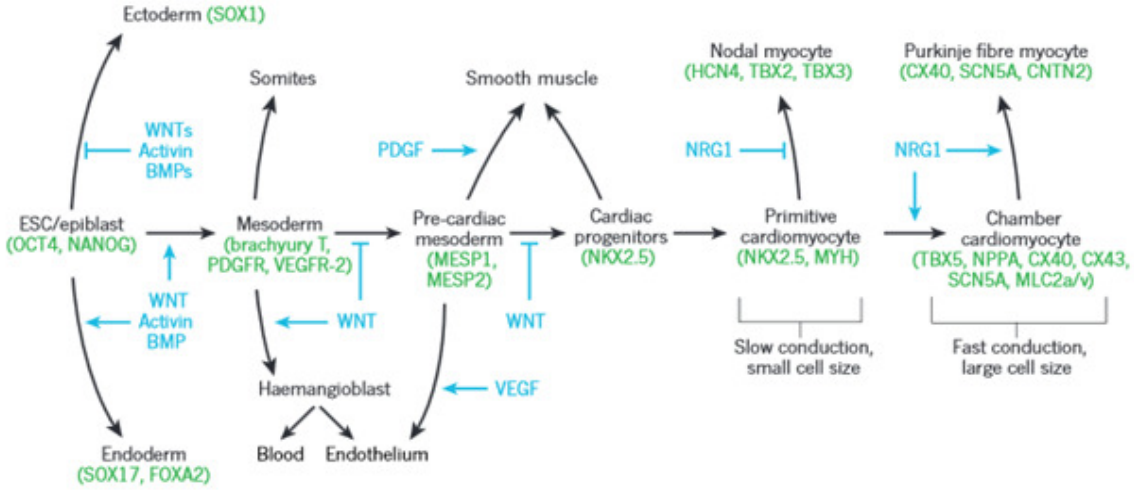

Fig. 5 Steps toward differentiation of cardiomyocytes (Laflamme and Murry, 2011).

Yet, the factors and genes involved in the cardiomyocyte differentiation are known only in part, among them an essential role has been shown to belong to the family of Bone morphogenic proteins

(BMP). They are a class of proteins directly involved in cardiogenesis, which play a key role in the early stages of differentiation, through the activation of the family of fibroblast growth factors (FGF), which in turn induce the expression of typical cardiac proteins (Behfar et al., 2002).

Another important family in cardiomyogenic differentiation is TGFβ. TGFβ2, in particular, has been associated with an increase in contractile embryoid bodies (Singla and Sun, 2005).

The Wnt proteins show a controversial role in the cardiac differentiation. They were initially considered suppressive of cardiac development, but activation effects have also been reported. Specifically, the non-canonical Wnt seems to enhance cardiac differentiation by the activation of protein kinase C (Koyanagi et al., 2005). The 'canonical' Wnt pathways, on the contrary, inhibit cardiac differentiation through the localization of β-catenin in the nucleus, promoted in turn by the inhibition of GSK3 (Gessert and Kuhl, 2010).

Greber and colleagues found that cardiac induction is promoted by the combined signaling activity of Wnt and BMP during the early stages of differentiation, both reducing the expression of pluripotency gene SOX2 and promoting the expression of mesodermal marker as the homeobox genes MSX1, CDX2, and CDX1 (Rao et al., 2016).

Also, BMP signaling is crucial in the regulation of the transcription factors Smad, which directly activates Nkx2.5 expression, early marker of the cardiac lineage (Brown et al., 2004).

Of note, in analogy to what observed in the developing heart, differentiating CMs obtained from ESCs express the cardiac transcription factors GATA4, Nkx2.5 and Tbx5 (Hiroi et al., 2001, Laemmle et al., 2016, Moskowitz et al., 2007, Neri et al., 2011, Sepulveda et al., 1998). Gata4 is necessary to establish, along with BMP, a positive loop to maintain Nkx2.5 expressions (Liu et al., 2009). In turn, Nkx2.5 has been shown to be necessary for efficient myocardial differentiation (Lyons et al., 1995, Tanaka et al., 1999) and, together with Tbx5, plays a fundamental role for the development of conduction system (Jay et al., 2004, Moskowitz et al., 2007) and chamber septation (Molkentin et al., 2000). Markers of mature cardiomyocytes such as cardiac troponin I and T, atrial natriuretic peptide (ANP), and atrial and ventricular myosin light chains (MLCs) also are expressed in mESC-derived CMs (Mauritz et al., 2008).
A detailed description of mESC-derived CMs, in comparison with freshly isolated adult CMs, will be reported in the following paragraph.

4.4 Properties of ES derived cardiomyocytes

The embryonic stem cell- derived cardiomyocytes (ESC-CMs) are a powerful tool used in various research areas including genetics and the screening for potential new drugs. However, although the quality of this model has been widely accepted, it should be never forgotten that significant differences exist between ESC-CMs and adult cardiomyocytes, the ESC-CMs being more similar to fetal/embryonic CMs (Pal, 2009, Vidarsson et al., 2010).

More in detail, it has been reported that ESC-CMs structurally and morphologically resemble embryonic or fetal cardiomyocytes (Youm, 2016). However, while adult CMs are large and cylindrical (approximately 150 × 10 μm for ventricular cells) (Lieu et al., 2009), early human pluripotent stem cell-derived cardiomyocytes (hPS-CMs) seen at the ignition of contraction are small and round, approximately 5–10 μm in diameter (Gherghiceanu et al., 2011, Snir et al., 2003, Boheler et al., 2002). Late hPS-CMs (>35 days), although acquiring a more oblong morphology remain small compared to adult (Snir et al., 2003). Further, ESC-CMs are mono-nucleated, while the majority of adult CMs present two or more nuclei (Smolich, 1995).

From an electrophysiological point of view, ESC-CMs in their early maturation phase exhibit contractile properties and embryonic like electrophysiology (i.e., small negative membrane potential and small action potential amplitude) (Erokhina et al., 2005, Horigome et al., 2000, Porrello et al., 2011). The longer they are kept in culture, the more mature is their electrophysiology (Cowan et al., 2004). In contrast to what observed in adult CMs, ESC-CMs exhibit spontaneous and synchronous contraction that can be maintained for more than 1 year in culture (Otsuji et al., 2010). The beating frequency of contraction may be affected by cell line, culture conditions and time since differentiation (Bilic and Izpisua Belmonte, 2012, Brito-Martins et al., 2008, Gupta et al., 2010, Reppel et al., 2004, Zhang et al., 2009).

The major ionic currents normally present in adult CMs are expressed in hPS-CMs, though frequently at abnormal levels (Robertson et al., 2013).

In ESC-CMs, the principal expressed channels during all the processes of differentiation are the alpha-subunit of a calcium channel (CaV2.1) and the T-type Ca^{2+}-channel; they are already present at the early stage (Maltsev et al., 1994) of differentiation and together are responsible for the intracellular fluctuations of Ca^{2+} current, that permit the spontaneously contraction (Viatchenko-Karpinski et al., 1999).

Importantly, the potassium currents considered to be responsible for arrhythmias in the adult heart are expressed in ESC-CMs (Caspi et al., 2009, Lahti et al., 2012, Wang et al., 2011). Thus, the use of ESC-CMs for drug screening is now widely applied (Braam et al., 2010, Dick et al., 2010, Tanaka et al., 2009, Yokoo et al., 2009), although arrhythmia development affected by time in culture (Sinnecker et al., 2013, Sinnecker et al., 2014)

In contrast to adult CMs, ESC-CMs have very little SR function in the early phase of differentiation and demonstrate calcium transients smaller and slower than adult CMs (Kang et al., 2012). Of note, calcium handling appears to vary significantly between lines (Robertson et al., 2013)

As reported before, RyRs have a remarkable expression in adult cardiomyocytes and they are also involved in a process called Ca- induced Ca^{2+} release (Woodcock and Matkovich, 2005), while the heart rate RyRs-dependent was confirmed at the early stage of differentiation in a CMs derived mESCs in RyR2 null model created by FU and colleagues, who showed a reduced frequency of Ca^{2+} transients and contractions(Fu et al., 2006a). The completed block of the contraction was permitted by the inhibition of SERCA2A, using the thapsigargin (Fu et al., 2006b).

Moreover, only the cells at the early stage of differentiation are able to continue to contract in the presence of a saturated solution of K +, while at the terminal stage of maturation, the contraction in the same solution is blocked, demonstrating that the calcium handling undergoes changes in the differentiation process. (Fu et al., 2006b).

At an early-stage of differentiation (30 day) when myocytes appeared, the myofibrils have a low density and the subcellular organization is irregular, while at a late stage (100 day) the sarcomeres are clearly visible with a traverse- tubular system (Lundy et al., 2013).

Finally, it is important to emphasize that exist a cell line-dependent variation of electrophysiological and morphology properties of ESC-CMs (Hannes et al., 2015).

5. *Haploid Mouse embryonic stem cells (mESCs)*

Mammalian cells possess two copy of each chromosome, a condition called diploidy. The diploid genome causes difficulties in generation of homozygous mutants, which are necessary for the study of recessive traits. In fact, if only one allele is disrupted, the resulting mutant might not exhibit the desired phenotype due to the compensation in protein expression caused by the transcription/translation of the second copy of the autosomal gene (Horii et al., 2013).

The fact that yeast possess a haploid genome has made these cells a widely used tool for genetic testing (Mable and Otto, 2001). Nevertheless, since the 1970s, large efforts have been made to generate haploid embryos in the mouse (Shuai and Zhou, 2014). Haploidy in mammals is restricted to germ cells, which do not survive *in vitro* long enough for genetic manipulation (Shuai and Zhou, 2014). Therefore, the establishment of a haploid mouse ESC line performed by different groups in recent years (Elling et al., 2011, Hong, 2010, Kaufman et al., 1983, Leeb and Wutz, 2011, Yang et al., 2012, Yi et al., 2009, Ying et al., 2008) potentially represents a great achievement for the advancement of genetic screening.

The mouse haploid ESCs that have been used in the present work have been kindly provided by the group of Prof. Joseph Penninger (Vienna). In 2011 Elling and coworkers produced haploid mouse embryos from parthenogenetic oocytes (Elling et al., 2011). Briefly, although the majority of the cells obtained from parthenogenetic embryos possesses a double copy of each chromosomes, the researchers of Penninger's group hypothesized that haploid cells should have been present in the blastocysts of parthenogenetic embryos obtained from C57BL/6J mouse strain. Therefore, after blastocysts collection, cells were dissociated, amplified under conditions able to maintain their undifferentiated state and sorted by FACS to obtain two independent haploid mESCs population (Elling et al., 2011). Importantly, haploid mESCs share important features with diploid ES cells, specifically being able to grow indefinitely in culture and to differentiate into cell types of the three gem layer, including cardiomyocytes (Elling et al., 2011). Of note, even if the haploid status is maintained only for the first stages of differentiation, the double haploids are also homozygous. This makes haploid mESCs a valuable tool to track the recessive phenotype in mice. In fact, with this model, it is possible to silence gene expression by performing a single event of insertional mutagenesis. The gene trapping is one of the most commonly used technique of insertional mutagenesis and it has been used to generate the mutants used in the present work.

5.1 Generation of mutant haploid mESC by gene trapping

Gene trapping is a method to introduce insertional mutations into genes (Gentile et al., 2003). It is specifically designed to disrupt gene function and can be used in large scale ES mutant production (Friedel et al., 2005). This technique usually relies on the random insertion of a reporter throughout the genome to create fusion proteins with a marker such as lacZ or GFP. It depends on the use of the so-called trap vectors, consisting of the reporter gene and/or selectable genetic marker flanked by an upstream 3' splice site (splice acceptor; SA) and a downstream transcriptional termination sequence (polyadenylation sequence; polyA). The gene trap cassette can be introduced into target cells using retroviral vectors or electroporation (Friedel and Soriano, 2010). When inserted into an expressed gene, the gene trap cassette is transcribed from the endogenous promoter of that gene in the form of a fusion transcript in which the exons upstream of the insertion site are spliced in frame to the reporter/selectable marker genes. Since transcription is terminated prematurely at the inserted polyadenylation site, the processed fusion transcript encodes a truncated and non-functional version of the cellular protein and the reporter/selectable marker. The shorter and less stable mRNA is then degraded, thus creating a loss of function mutant (Fig. 6) (Broso F., Tesi di Laurea, 2014).

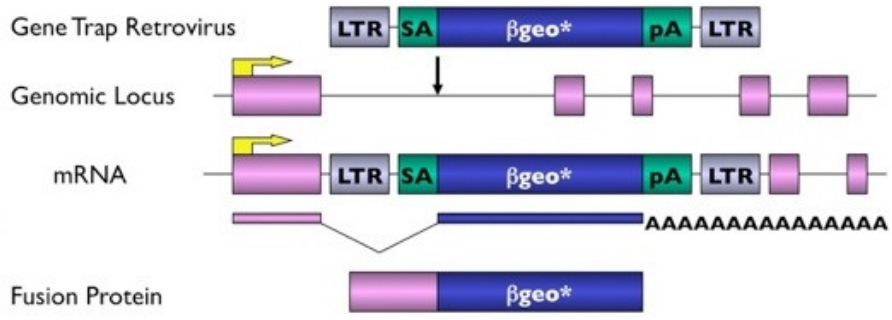

Fig. 6 Gene-trap vector (from http://research.mssm.edu/soriano/lab/gene_trap.html).

A library of haploid mESCs characterized by gene trap insertion in single genes has been created in the laboratory of Prof. Joseph Penninger, at the Institute of Molecular Biotechnology (Vienna, Austria). The gene trapping cassette was inserted into a lentiviral vector containing the beta-galactosidase reporter and Neomycine resistance as selection maker. The vector also contained removable Oct4 binding sites, allowing the insertion in genes minimally expressed into mESCs (Elling et al., 2011). The insertional mutagenesis was successful in producing the Striatin gene loss in two cell lines. One of these, called 377C05, was used in the present work.

As show in the Fig. 7, in the 377C05 mutant, the Striatin gene was stopped after 511aa and missing part of the WD-repeat domain. As control, the relative wild type line (called AN3) was also provided.

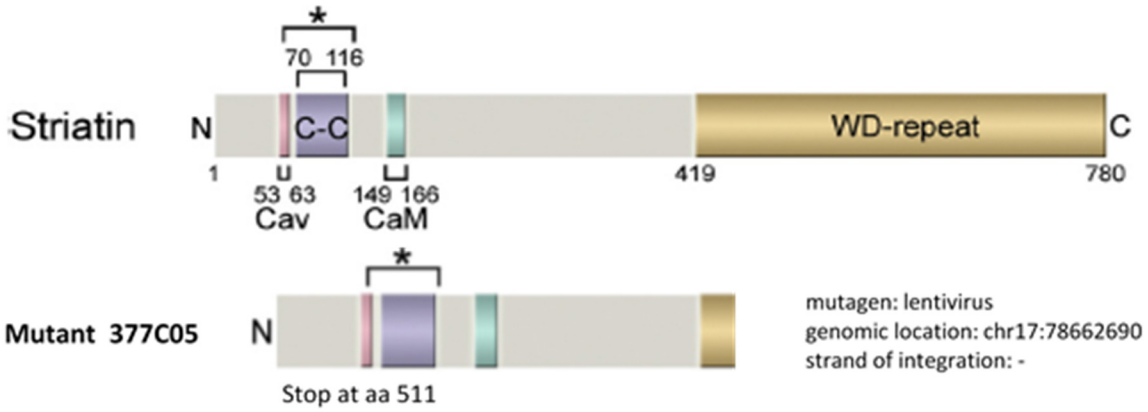

Fig. 7 Striatin and mutant: modified from (Cambier et al., 2014, Hwang and Pallas, 2014)

Preliminary evidence and aim of the work

The present work of thesis is part of a wider project conducted in our laboratory. As outlined in the introduction, the haploid mESC wild type (WT AN3) mutant cell line (377C05) used in the present work was kindly provided by Prof. Joseph Penninger group (IMBA, Vienna).

The confirmation insertion site position and orientation of the mutagenesis cassette in the line 377C05 has been done previously in the Laboratory of Prof. Penninger and is not part of the work presented here (Penninger et al; unpublished data).

Preliminary experiments performed by Piubelli C. and Broso F. (Broso F., Tesi di Laurea, 2014) indicates that, as expected, the 377C05 mutants lack Striatin both at the mRNA and the protein level.

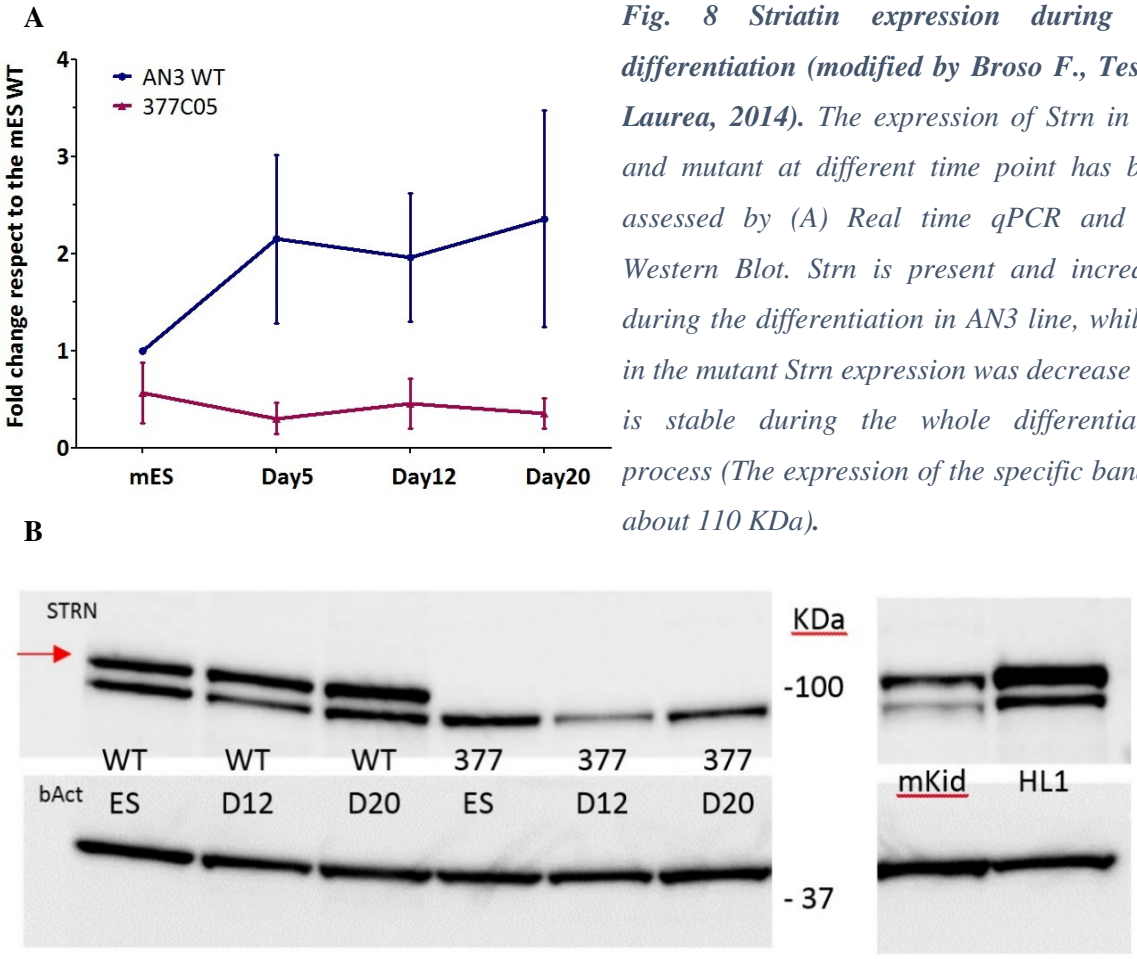

Fig. 8 Striatin expression during the differentiation (modified by Broso F., Tesi di Laurea, 2014). *The expression of Strn in WT and mutant at different time point has been assessed by (A) Real time qPCR and (B) Western Blot. Strn is present and increases during the differentiation in AN3 line, while is in the mutant Strn expression was decrease and is stable during the whole differentiation process (The expression of the specific band at about 110 KDa).*

Further, it has been reported that 377C05 mutants exhibit a different Nkx2.5 expression and a significant delay in the appearance of beating areas compared to the WT. This seemed associated with an increase in the spontaneous beating and contraction frequency of the mutants. However, the work performed by Piubelli C. and Broso F. (Broso F., Tesi di Laurea, 2014) was still preliminary and characterized by a low number of independent observation in electrophysiology experiments (n=2).

Aim of the present work was to characterize in depth the electrophysiological alteration of 377C05 mutants, therefore confirming a potential role for Striatin as a new player in cardiac disease.

Materials and Methods

6. *Haploid mouse stem cell culture*

Striatin-mutant (377C05) and wild-type (AN3) mESCs were kindly provided by Prof. Penninger lab at IMBA (Vienna) as frozen aliquots.

After thawing, haploid mESCs cells were resuspended in 37°C ES cell culture medium (ESCM) composed as follows (Broso F., Tesi di Laurea, 2014):

Reagent	**Cat. No**	**Volumes for 550 ml**
DMEM	Gibco 42430	450 ml
FBS	Gibco 10270	75 ml (13, 63%)
Penicillin Streptomycin	Gibco 15070-063	5,5 ml (100X)
Nonessential amino acids	Gibco 11140-035	5,5 ml (100X)
L-Glutamine	Gibco 25030-081	5,5 ml (100X)
Sodium Pyruvate	Gibco 11360-039	5,5 ml (100X)
β-mercaptoethanol	Gibco (stock 50 mM)	520 µl (1000x)
LIF	CHEMICON International	10 units/ml

Resuspended mESCs were then centrifuged at 300 rcf for 5 min to remove DMSO traces, plated onto a MEF feeder layer in 6 multi-well plates and placed in a humidified incubator gassed with 5% CO2 at 37°C

Of note, for the present work undifferentiated mESCs were cultured on a Mouse Embryonic Fibroblasts (MEF) feeder layer, instead of simply amplified on plastic as described in Ulling et al, and in Broso F. (Broso F., Tesi di Laurea, 2014). This allowed us to increase the amount and the dimension of beating areas compared to what reported in Broso F. (Broso F., Tesi di Laurea, 2014).

In particular, MEF mitotically arrested by irradiation (Global Stem) were plated onto 0.1% gelatin (Millipore) coated 6-well plates plate, at a density of 2 x 10^5 cells/well one day before passaging the mESCs.

After reaching a 75%-85% of confluence, the cells were washed with 2 ml/ wells of Phosphate Buffered Saline (PBS – Gibco). One ml of 0.05% Trypsin-EDTA 1X (Gibco) was then added to the wells and the cells were left 3 min in the incubator at 37 °C to allow their detachment from the surface. To inhibit the trypsin effect 2 ml of ESCM were added and the cell suspension was then centrifuged for 5 min at 300 rcf. The supernatant was discarded and the pellet resuspended in about 3 ml of ESCM to dilute the cells and to obtain the appropriate cell density for seeding (1.0 X 10^6 or 1.8 x 10^6 cells per well in a 6-well plate). For an efficient maintenance of stem cells, it is important to uphold a correct density, since a too high density encourages random differentiation. The splitting of cells was done every 3-4 days depending on the growth rate of cells.

7. *In vitro cardiomyogenic differentiation by the hanging drop technique*

The protocol used to obtain cardiomyocytes from mouse haploid stem cells is summarized in Fig. 9. It basically promotes the spontaneous differentiation of haploid mESCs, by removing Leukemia Inhibitory Factor (LIF) and increasing the serum percentage in the culture medium (Hussain et al., 2013).

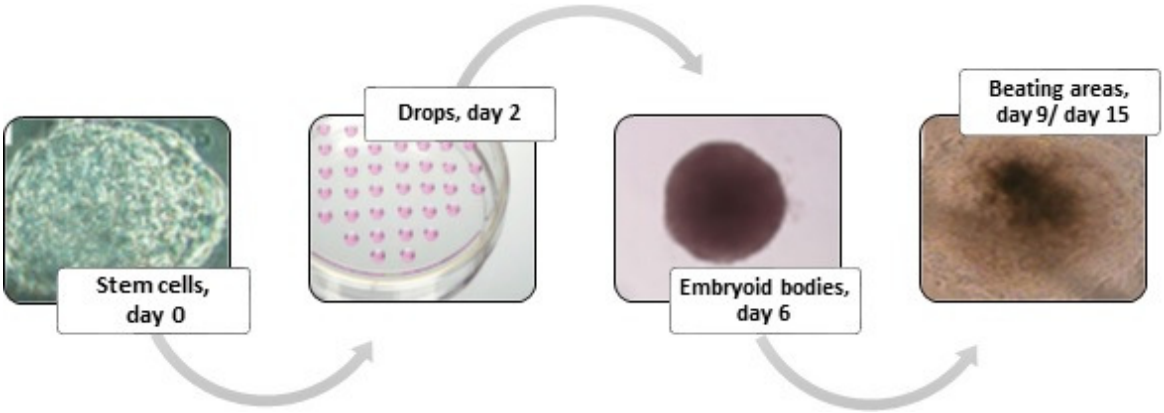

Fig. 9 Mouse haploid ES differentiation workflow

Before starting with the differentiation protocol, mouse embryonic fibroblasts were removed by aspiration, under the dissecting microscope, thus ES cells were differentiated by the "hanging drop" method.

In detail, as described by Wobus and colleagues (Wobus et al., 2002), the undifferentiated stem cells were dissociated as single cells by Trypsin treatment, as described above for splitting, and resuspended in the differentiation medium, consisting of ESCM deprived of LIF and supplemented with 20% FBS. Notably, the cells were counted and diluted to a final concentration of 66000 cells/ml. This allowed the formation of 30 µl drops, each containing approximately 2000 cells, a higher number compared to the current literature (Wang and Yang, 2008, Wobus et al., 2002, Boheler, 2003), but necessary for us to promote an efficient cardiomyogenic differentiation from haploid mESCs (Broso F., Tesi di Laurea, 2014). Approximately 80 drops were placed on the undersurface of a 100 mm Petri dish lid (Kord-Valmark Disposable Polystyrene Petri Dishes). Finally, to prevent the drops to evaporate, the plate was filled with PBS and incubated at 37 ° C and 5% CO2.

After 2 days, the drops were collected and the embryoid bodies left to grow in suspension in a low attachment petri (Kord-Valmark Disposable Polystyrene Petri Dishes), in order to enlarge the spheroidal dimensions of the three-dimensional embryoid bodies (EBs) for other 4 days in incubator with fresh differentiation medium.

At day 6, the EBs were transferred into 6-wells-plate previously coated with 0.1% gelatin solution (Millipore), which facilitates the adherence of the embryoid bodies to the plate surface.

The plastic adherent EBs were then left to spontaneously differentiate. The first beating areas usually appeared at day 9. New beating areas usually appeared until day 12-13. As previously described (Zhou et al., 2003) we observed the progressive disappearance of spontaneous beating at day 14-15.

8. *Gene expression analysis*

For gene expression analysis, total RNA was extracted from beating areas, manually dissected with a needle as described above, at two time points: day 0 (corresponding to undifferentiated stem cells) and day 12 of differentiation. The methods used for RNA extraction and quality check, cDNA preparation and Real-Time RT-PCR has been already described in Broso et al. (Broso F., Tesi di Laurea, 2014)

8.1 RNA extraction and quality check

Qiagen RNeasy Plus Mini Kit was used as the instructions in the manual with the use optional of DNAse digestion. In case of RNA isolation from micro-dissociated beating areas, after lysis, the lysate was passed through a needle for several times before subsequent steps according to the instruction manual.

The actual amount of RNA present in the final solution was measured through the NanoDrop 1000 Spectrophotometer, which also evaluates the purity of the sample by calculating the ratio of the wavelength of 260 nm and 230 nm and between 260 nm and 280 nm.

Furthermore, the integrity of the extracted RNA was assayed by an electrophoretic technique, with the Experion ™ Automated electrophoresis station and the related experimental kits Experion ™ Reagent SdtSens and Chips produced by BIO-RAD.

The results shown from the software identify three peaks; the first is the marker followed by the peaks for 18S and 28S ribosomal RNA (rRNA); a size and a concentration are then assigned to these peaks. The software automatically generates a RNA quality indicator value, comparing the area of the peaks corresponding to the rRNAs the system evaluates. More the RQI is lower, more the RNA was highly degraded, while for an intact RNA the result is 10. For our experiment an RQI less than 8 was considered not acceptable

8.2 cDNA preparation

1000 ng of total RNA was reversely transcribed using SuperScript® VILO cDNA Synthesis Master Mix in 20µl volume. The thermal cycle was set as follow: primer annealing at 25 ºC for 10 minutes,

then reverse transcription at 42 ºC for 1 hours, and finally denaturation of the enzyme at 85 ºC for 5 minutes. The final cDNA products were stored at -20 ºC until further use.

8.3 Real Time –PCR

cDNA was amplified by All-in-One qPCR mix according to the manufacturer's instructions. Quantitative RT-qPCR was performed on CFX96™ Real Time PCR with the conditions as follows: one step of 95°C for 1 min, and 45 cycles of 95°C for 10 s denaturation and a step of annealing from 55°C to 60°C for 20 second each and a finally extension phase at 72°C for 15 sec.

The threshold cycle number for product detection (ΔCT value) was used to calculate the relative expression levels. Relative quantitation was performed using the ΔΔCt method. Fold changes in gene expression were estimated as 2(-ΔΔCt)

For the pluripotency marker analysis, we used as normalizer the expression of each pluripotency gene at baseline in the WT undifferentiated ES cells. For the other genes (cardiac, ion channels and Striatin-interaction protein), the normalizer was the median expression value of each single gene at day 12 of WT *in vitro* differentiation.

As previously described from Piubelli C. and Broso F. (Broso F., Tesi di Laurea, 2014) a NormFinder software was used to identify the optimal normalization gene among five candidate housekeeping gene; Hypoxanthine Guanine Phosphoribosyl Transferase (HPRT) resulted as the most suitable housekeeping gene for our study. For this reason, HPRT is the reference gene used for all experiments (Broso F., Tesi di Laurea, 2014), while cDNA from adult mouse heart was used as a positive (or negative for pluripotency genes) control.

8.4 List of used primers

GROUP	REFERENCE SEQUENCE	TARGET GENE AND SEQUENCE
PLURIPOTENCY MARKERS	NM_013633.3	mOct4-F: TCAGGTTGGACTGGGCCTAGT
		mOct4-R: GGAGGTTCCCTCTGAGTTGCTT
	NM_011443.3	mSox2-F: GGCAGAGAAGAGAGTGTTTGC
		mSox2-R: TCTTCTTTCTCCCAGCCCTA
	NM_028016.3	mNanoG-F: GAAATCCCTTCCCTCGCCATC
		mNanoG-R: CTCAGTAGCAGACCCTTGTAAGC
HOUSEKEEPING GENES	NM_008084	mGAPDH-F: CCTCGTCCCGTAGACAAAATG
		mGAPDH-R: TGTAGTTGAGGTCAATGAAGGG
	NM_013556	mHPRT-F: GCCCTCTGTGTGCTCAAG
		mHPRT-R:CCCCGTTGACTGATCATTACA
	NM_013684	mTBP-F: TCAAACCCAGAATTGTTCTCC
		mTBP-R: AACTATGTGGTCTTCCTGAATCC
CARDIAC DIFFERENTIATION MARKERS	NM_008700.2	mNkx2.5-F: ACTTGAACACCGTGCAGAG
		mNkx2.5-R: GTCATCGCCCTTCTCCTAAAG
	NM_010856.4	mMyh6-F: GCAGAACAGTAAAATTGAGGACG
		mMyh6-R: CGCAGCTTCTCCACCTTAG
	NM_080728.2	mMyh7-F: CCATCTCTGACAACGCCTATC
		mMyh7-R: GGATGACCCTCTTAGTGTTGAC
	NM_010861	mMyl2-F: AGCCTTCACAATCATGGACC
		mMyl2-R: AAGTTAATTGGACCTGGAGCC
ION CHANNELS	NM_010408.3	mHCN1-F: GGCGAGGTCATAGGTCATGT
		mHCN1-R: CGCCTTTCAAGGTTAATCAGA
	NM_008226.2	mHCN2-F: GCTCATCCGATATATCCACCA
		mHCN2-R: CTTGCCAGGTCGTAGGTCAT
	NM_001081192.1	mHCN4-F: GTGGGGGCCACCTGCTAT
		mHCN4-R: GTCGGGTGTCAGGCGGGA
	NM_008425.4	mKCNJ2-F: TGAAGTTGCCCTAACAAGCA
		mKCNJ2-R: GCTCTCTGGGACTCCGTTCT
	NM_009781	mCacna1c-F: TGTCCCTCTTCAACCGCTTTGACT
		mCacna1c-R: GTTCAGCAAGGATGCCACAAGGTT
	NM_021544.3	mSCN5A-F: AGCAGGGCTGGAATATCTTCGACA
		mSCN5A-R: GCCATGATTTGGCCAGCTTGAAGA
	NM_023868.2	mRyR2-F: TTCAACACGCTCACGGAGTA

		mRyR2-R: GTGCCAGGCTCTGCTGAT
	NM_001110140.3	mATP2A2-F: GTTGGTGACAAAGTTCCTGC
		mATP2A2-R: TGTCTTGATTAACAGCTCGGG
STRIATIN	NM_011500	mSTRN-F: ACAGGCACATCAAGTTCTACG
		mSTRN-R: ACATCAAGTAGAGGCCATTCG
STRIATIN-INTERACTING PROTEINS	NM_001165902.1	mCTNNB1-F: TGCAGATCTTGGACTGGACA
		mCTNNB1-R: AAGAACGGTAGCTGGGATCA
	NM_010288.3	mGJA1-F: GCTTGGCGTGTTCTTCAATCC
		mGJA1-R: ACTCCTGTACTTGGCTCACGT
	NM_011578.3	mTGFBR3-F: TGCTGGAGTGGTAGTGTTTAAC
		mTGFBR3-R: TGACAGACACCTCAACATATACA
	NM_028351.3	mRSPO3-F: TGTACAAAATGCAAAGTTGACTG
		mRSPO3-R: TGGCCTCACAGTGTACAATA
	NM_009756.3	mBMP10-F: CATCCGGAGCTTCAAGAACG
		mBMP10-R: TTGATGGGCCTGACTTTTGC
	NM_016891.3	mPPP2R1A1-F: CCTCTTGCCCCTGTTCTTG
		mPPP2R1A1-R: CTTCAGCTAGTTCCACGATGG

9. *Embryoid body dissociation.*

At day 12, beating areas from control and Strn-mutants were manually dissected with a needle under the dissecting microscope in the picking-hood after 12 days of differentiation

Approximately 15-20 of these micro-dissociated beaters were seeded on 0.1% Matrigel-coated 35mm dishes and use after 48h for electrophysiology recording; while the remaining was used for Real-Time PCR.

About 30 micro-dissociated EBs for each experiment were further dissociated in small cell aggregates and single cells to be used for immunofluorescence analysis and calcium imaging experiments. In detail, EBs were collected, washed with 1 ml of PBS, centrifuged at 500 rpm for 5 min and enzymatically dissociated by incubation with 1 ml of TripLE ™ Express (Gibco) for 10 min at 37 °C. EBs dissociation was mechanically completed by pipetting the suspension for several times. The enzymatic activity was then inhibited by adding 1 ml of fresh differentiation medium containing 20% FBS. Isolated cells and small aggregates were finally centrifuged at 500 rpm for 5 min, resuspended in differentiation medium and were seeded on 0.1% Matrigel-coated 60µ-dishes uncoated (IBIDI).

10. *Video Analysis*

Nineteen spontaneous beating EBs were video recorded in an AVI video file for each one of 5 independent differentiation experiments carried out in parallel for 37705 mutants and WTs. Their contractile properties were then analyzed by Dr. Lorenzo Fassina using the Video Spot Tracker (VST) program (Fassina et al., 2011), which allows to track the motion of one or more spots in each video. 30 spots or markers were systematically selected onto the first video frame of each video, according to the same orthogonal grid. By starting the videos in VST, frame by frame, the program followed and registered the spatial-temporal coordinates x, y, and t for each marker, as previously described (Fassina et al., 2011). The coordinates x and y are expressed in [pixel], whereas the coordinate t is expressed in[s]. Successively an algorithm was ameliorated in order to filter, that is, to exclude the tracking components at high frequencies (f>10 Hz), which are not culture beats, but noise. In particular, the de-noising was performed via wavelet compression (near symmetric wavelet: Symlets

4; decomposition level: 3; compression method: global threshold leading to recover 99% of the track energy).

11. *Electrophysiology and Calcium Imaging*

11.1 Electrophysiological recordings

In order to evaluate the effects of the Striatin deficit on the spontaneous capacity of the cardiomyocyte to generate action potentials and their characteristics, manually dissociated whole EBs were placed in a sample-carrier chamber thermostatically controlled at 36°C–37°C, mounted on the work surface of an inverted microscope (Nikon Eclipse Ti-U; Nikon, Japan). Throughout the recording, the biological preparations were perfused with the High Glucose Tyrode solution, with the following composition:

	g /L	Final concentration in mM
D(+)-glucose	4.5	25
Hepes	1.192	5
Sodium Chloride (NaCl)	8.176	140
Potassium chloride (KCl)	0.402	5.4
Magnesium Dichloride ($MgCl_2$)	0.244	1.2
Calcium Dichloride ($CaCl_2$)	0.200	1.8

pH adjusted to 7.3 with NaOH

The microscope was placed inside a Faraday cage and in bearings on an anti-vibration table in order to ensure both electrical insulation and environmental vibrations.

The patch pipettes obtained from borosilicate glass capillaries (BF150-86-10 Sutter Instrument,); by using a horizontal puller (Sutter model P-1000, Sutter Instrument, USA) displayed a tip resistance of 5-9MΩ when filled with an intracellular solution composed by:

	g/50mL	Final concentration in mM
K-aspartate	1.113	130
Hepes	0.120	10
Sodium ATP (Na-ATP)	0.138	5
EGTA	0.210	11
Sodium GTP (Na-GTP)	0.003	0.1
Calcium Dichloride ($CaCl_2$)	0.555	5
Magnesium Dichloride ($MgCl_2$)	0.190	2

pH adjusted to 7.2 with KOH

The pipettes, once filled with the intracellular solution, were mounted on a holder and approached to the selected cell by a micromanipulator which allows movements in the order of a few microns. When the pipette tip contact the cell membrane (cell attachment configuration) the glass of the pipette establishes chemical bonds with the membrane phospholipids and this translates into an increase in electrical resistance, given by the sum of the pipette and the membrane resistance (some GΩ); this is referred as a Gigaseal.

Subsequently, by means of a syringe connected at holder, it makes a small suction, which allows to break the fragment of underlying membrane, sealing it to the tip of the pipette. In this way, an electrical continuity is achieved between the interior of the pipette and the cell interior ('whole-cell' configuration).

Any current which flows from the pipette is now forced through the whole cell membrane and, the measured potential difference is the one between the inside and the outside of the cell (by a reference electrode present in the sample-carrier chamber). The recording microelectrode and the reference electrode were connected through an amplifier interfaced with a computer.

11.2 Current-clamp recordings

In our experiments the spontaneous cellular electrical activity was recorded using the whole-cell configuration in the current-clamp mode.

In this technique, the membrane potential is free to vary, and the amplifier records whatever voltage the cell generates on its own (spontaneous) or as a result of stimulation (evoked).

Spontaneous cardiac action potential (APs) were recorded at physiological temperature (33–35°C) using a Multiclamp 700B amplifier (Molecular Devices, LLC). Data acquisition was performed using pClamp 10.0 software and the Digidata 1550 interface (Molecular Devices, LLC). Data were filtered at 3 kHz and sampled at 10 kHz.

The analysis of the data was carried out by using Clampfit 10.0 (Molecular Devices, LLC) in combination with GraphPad Prism software 6.03, Microsoft Excel and the home-made software ClampMatic, to calculate the following parameters:

- the takeoff potential (**TOP**, mV), which is the minimum potential equivalent to the threshold value. It was automatically calculated by the software ClampMatic by considering the voltage at which the dv/dt value change significantly.
- the upstroke (**peak**, mV), which represents the maximum peak of the action potential;
- the maximum diastolic potential (**MDP**, mV); which represents the minimum peak of the action potential;
- the amplitude of the action potential (**APA,** mV), computed as the difference between MDP and the upstroke;
- the action potential duration at 20%, 60% and 90% of membrane repolarization phase (**APD 20- APD 60- APD 90,** ms). calculated as the elapsed time to obtain the X% of the APA from the time of the AP threshold.
- The inter-event-interval (**IEI**, ms) which is the elapsed time between the peak of an AP to the peak of the next one.

- The coefficient of variation of inter-event intervals (**CV-IEI**), which is the ratio between the standard deviation of the IEI and the mean value of the IEI ($CV_{IEI} = SD_{IEI} / MEAN_{IEI}$).

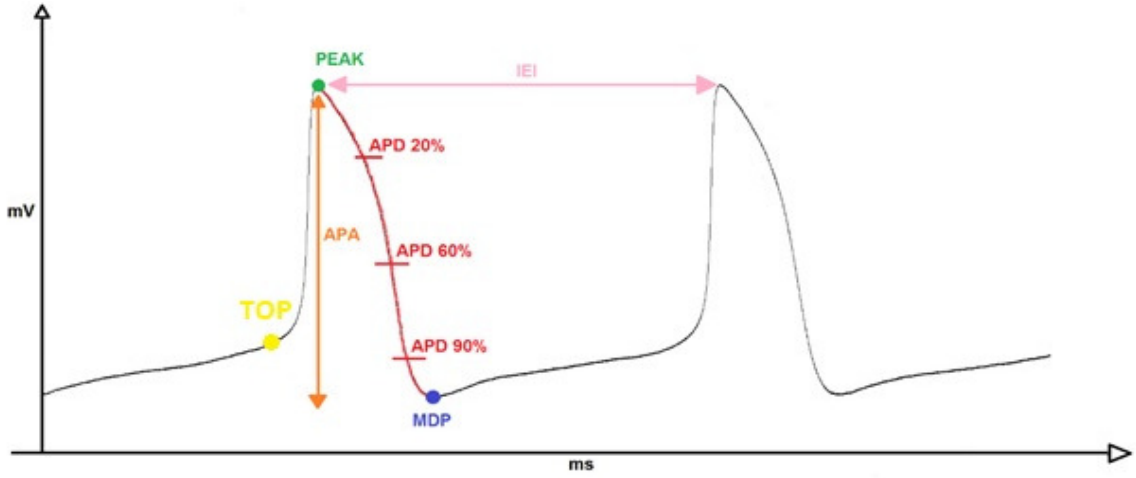

Fig. 10 Representative trace of recorded APs with all the calculated parameters.

11.3 Calcium Imaging

In order to study the calcium handling capacity of the obtained cardiomyocytes, the micro-dissociated EBs were loaded with Fluo-4-acetoxymethyl (AM)-ester. For this purpose, 1 µl of Fluo-4 was dissolved with 1 µl pluronic DMSO (Invitrogen) and 2.5mM Probenecid in 1ml of High Glucose Tyrode forming the fluo-mix and then the EBs were incubated in 1 ml (i.e. 500 µl of fluo-mix + 500 µl of Tyrode) for 20-30 min at 37°C in an incubator. After this, the culturing dishes were placed under the microscope in the sample-carrier chamber thermostatically controlled. -
To measure calcium signals, Fluo-4–loaded cardiomyocytes were excited at 488 nm and the emitted light was collected with a spectral detector from 520 to 620 nm through a 40X oil-immersion objective lens. The spontaneous activity of micro-dissociated EBs were recorded as a stream-acquisition for 60-120 sec. The images (696 x 520 pixels) were acquired at 20 Hz converted into a movie file by the Metafluo software and saved as a data file to allow the off-line analysis by combining Microsoft Excel and the home-made software CalciumStat. Fluo-4 fluorescence intensity is expressed as the F/F_0-ratio, where F is the background-subtracted fluorescence intensity and F_0 is the background-subtracted baseline fluorescence value measured at rest.

12. *Immunofluorescence*

After 48 h from disaggregation of embryoid bodies, the wild type and the Strn-mutant derived cardiomyocytes were washed twice with 1x PBS and fixed in 4% cold paraformaldehyde/1x PBS. The samples were kept at 4 °C until their usage.
Cardiomyocyte preparations, maintained at 4 °C, were washed twice with 1× PBS and permeabilized with 0.1% Triton X-100 in PBS for 10 min for the detection of cardiac troponin T. For these antibodies, an incubation with 5% Goat serum /PBS for 1 h at room temperature was performed to block non-specific protein-binding sites. Afterwards, cells were incubated with primary antibodies overnight at 4 °C.
After this, the cells were rinsed three times with PBS and incubated for 1 h at 37 °C using a secondary antibody diluted in PBS (AlexaFlour 555-conjugated anti-mouse IgG, 1:1000; Molecular Probes).

Primary antibodies

Target protein	Clone	Dilution	Incubation
Troponin T	Abcam ab8295	1:250	O/N at 4 °C

Secondary antibodies

Target protein	Clone	Dilution	Incubation
Alexa Fluor 555-conjugated goat anti-mouse	Molecular Probes, A-21422	1:1000	1h 37°C

After three washes with PBS, nuclei were counterstained with NucBlue Fixed cell Stain Ready Probes reagent.
Images were visualized with an TCS SP8 X Leica fluorescence microscope.
For each antibody and for each of the three independent experiments performed, a total of about 100 cells were photographed and analyzed by a software for digital image processing, ImageJ.

In case of RNA isolation from micro-dissociated beating areas, after lysis, the lysate The results shown from the software identify three peaks; the first is the marker followed by the peaks for 18S

and 28S ribosomal RNA (rRNA); a size and a concentration are then assigned to these peaks. The software automatically generates a RNA quality indicator value, comparing the area of the peaks corresponding to the rRNAs the system evaluates. More the RQI is lower, more the RNA was highly degraded, while for an intact RNA the result is 10. For our experiment an RQI less than 8 was considered not acceptable

Quantitative RT-PCR was performed on CFX96™ Real-Statistical analysis.

All the data were analyzed using non-parametric Wilcoxon tests. Results are reported as mean ± S.E.M. All statistical analyses were conducted using the statistical tool of GraphPad Prisms software 6.03.

12.1 One-sample Wilcoxon rank sum test

The Wilcoxon test for paired samples is the non-parametric equivalent of the paired samples t-test. It should be used when the sample data are not normally distributed, and they cannot be transformed to a normal distribution by means of a logarithmic transformation.
The null hypothesis (H0) sustains that the medians of all considered group are equal, while the alternative hypothesis (H1) says that at least one median of one group differs from that of at least another one.
One assumption of the test is that groups have an equal intragroup variability meaning they have the same distribution. It works on ranks, so the observations are converted into a ranking: the smallest value has rank 1, the next one will be 2 and so on. This is done for each group. Then the test searches for differences in mean ranks to assess the null hypothesis.
The use of this test is recommended when there is one nominal variable and one measurement variable.
We rejected the H0 for p-values lower than 0.05, while the presence of a trend was considered with p-value lower than 0.10.

12.2 Two-sample Wilcoxon rank sum test

Also known as Mann-Whitney test, it is a nonparametric alternative to the two-sample t-test. It tests the null hypothesis that the distribution of the measurements in the sample A is the same as that in B. In other words, it verifies if the measurements of the two samples come from the same population and for this reason have the same probability distribution. In addition, this test is based upon ranking, so each observation has a rank. The null hypothesis is rejected for p-value lower than 0.05. P-values <0.10 indicating a trend of association.

Results

13. *Qualitative evaluation of cardiomyogenic differentiation*

The total amount of embryoid bodies generated by 377C05 mutants and WT was first counted at day 7 of differentiation, showing no difference between the two groups (Fig. 11). Mean values were 60 ± 12 (N=10) and 60 ± 13 (N=12) for WT and mutants, respectively. This result indicates that the mutants retain the ability to form 3D differentiating structure. In 9 differentiation experiments, we also evaluated by microscopic inspection how many EBs harbored inside one or more spontaneously beating portion. Each beating area was marked and the count repeated from day 9 to day 13. The number of beating areas was then normalized on the total number of EBs to obtain the percentage of beaters.

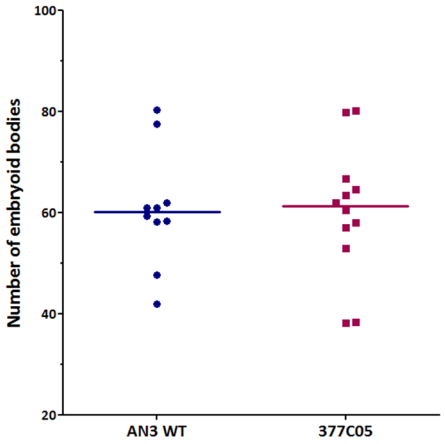

Fig. 11 Number of embryoid bodies *Embryoid bodies number was count for 10 (in WT) and 12 (377C05) independent differentiation experiments. No significant difference was demonstrated.*

Average % of beating areas (N=9)	
AN3 WT	**377C05**
97%	71%

Table 2 The total number of beating areas for cell line was normalized on the total number of EBs. *From day 9 up to day 13, total beating areas for 9 different experiment was counted.*

These experiments showed a consistent reduction in the number of developed beating areas in 377C05 with respect to the WT at day 12 (Fig. 12). The data are plotted using box plots, medians and interquartile range were used as descriptive measures; it has to be considered that EBs can harbor inside two or more spontaneous beating portion: for this reason, the box plot of WT line is larger than 100%. The test used to compare the groups, considering six differentiation experiments, was a non-parametric Wilcoxon rank-sum test (also known as Mann-Whitney test), which gave a P value=0.0303. These results confirm the preliminary evidence reported by Piubelli C. and Broso F. (Broso F., Tesi di Laurea, 2014).

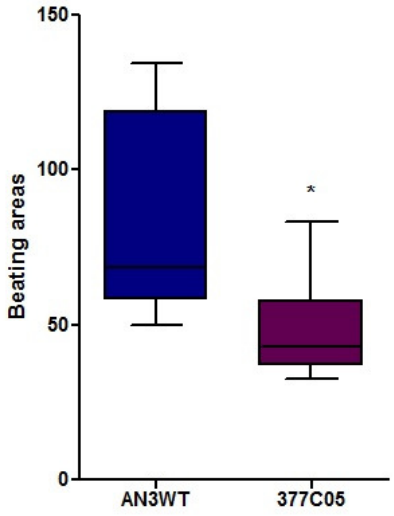

Fig. 12 Percentage of new beaters at day 12 in mutant vs WT. *In N=5 for WT and n=6 for 377C05 differentiation, the mean percentage of beating area appeared at day 12 of differentiation was 84 ± 34 for the WT and 49± 18 for 377C05 mutant (p =0.0303; non-parametric Mann-Whitney test).*

Also at day 12, we noticed that the size of beating areas in the wild type was greater than in mutant. Then, the dimension of beating area (expressed in pixels) were captured and analyzed by ImageJ. Again, statistical differences were explored. In detail, nine videos from three independent differentiation experiments were investigated. Box plots show that beating areas in the WT are about three times bigger than in the mutant.

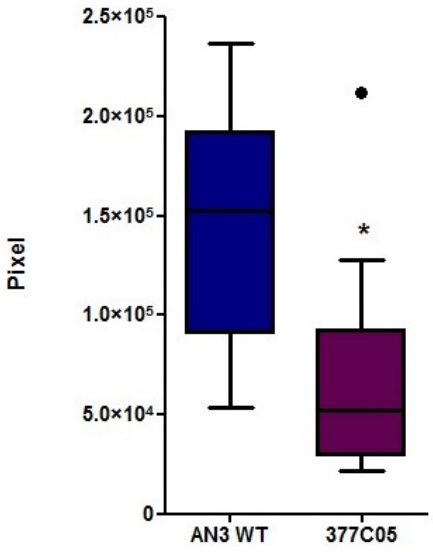

Fig. 13 Box plot of the dimension (in pixels) of beating areas measured at day 12 of differentiation. *Considering 9 videos from 3 independent differentiation experiments the mean dimension of beating area at day 12 of differentiation was* $1.4x10^5 \pm 2x10^4$ *for the WT and* $7x10^4 \pm 2x10^4$ *for 377C05 mutant, a non-parametric Mann-Whitney test gave a P value = 0.0142. In the mutant is present an outlier values indicated with a dot out from box plot.*

14. *Gene expression modulation*

Evaluation of Pluripotency and Cardiac Gene

RT-qPCR experiments were performed in order to evaluate whether the difference observed in the functional properties of 377C05 mutants was due to a different gene expression. We focused on two time points: day 0 (i.e. baseline – undifferentiated ES cells) and day 12 (i.e. time-point where differences on beating areas appeared).
We tested the expression of pluripotency gene, as their expression is expected to decrease during differentiation (Miyamoto et al., 2015), as well as a panel of early and late cardiac genes to evaluate cardiomyogenic differentiation. Finally, the expression of ion channels and Striatin-interacting protein genes was analyzed in order to evaluate possible pathways affected by the lack of Striatin.

Pluripotency markers

As expected, a decrease in the pluripotency genes were observed in both groups, being also similar in their proportions. The medians of the calculated fold-changes (FC) at each time point (i.e. day 0 and day 12) are reported in Table 3.

Gene	**Group**	**377 (day 0) FC median (IQR)**	**P value day 0 [1]**	**WT (day 12) FC median (IQR)**	**377 (day 12) FC median (IQR)**	**P value day 12 [2]**
NANOG	Pluripotency	0.97 (0.8-1.12)	0.711	0.57 (0.56-0.98)	0.69 (0.34-0.97)	0.8478
OCT4	Pluripotency	1.02 (0.67-1.37)	0.8129	0.48 (0.39-0.55)	0.48 (0.23-0.63)	0.9488
SOX2	Pluripotency	1 (0.71-1.19)	0.8606	0.82 (0.62-1.02)	0.77 (0.58-0.94)	0.5649

Table 3 Pluripotency gene expression analysis. *In N=7 independent differentiations, the expression levels of NANOG, OCT4 SOX2 were evaluated at day 0 (mESC) and day 12 of differentiation, in both cellular lines. For the 377 at day 0 One-sample Wilcoxon test was used ([1], non-significant*

difference observed). For the evaluation of both cellular lines at day 12 of differentiation Two-sample Wilcoxon text was used ([2], non-significant difference observed). The calibrator used in both analysis is WT at day 0.

Cardiac differentiation markers

It is expected that cardiac genes progressively appear according to the differentiation stage (Boheler et al., 2002). Additionally, the maturation of cardiomyocytes is accompanied by the expression of ion channels responsible for CMs electrical activity. Table 4 presents the results obtained for each analyzed gene expressed as the median of fold-changes with the relative IQR (i.e. interquartile range) reported. Data shown here are in contrast with those described by Piubelli and Broso (Broso F., Tesi di Laurea, 2014). Indeed, our results show a trend towards an upregulation of the early cardiac marker Nkx2.5, while Piubelli and Broso found lower Nkx2.5 expressions in the mutant (Broso F., Tesi di Laurea, 2014). The discrepancy can be explained considering that in this version of the work the RT-qPCR was performed using only the RNA extracted from manually dissected beating areas, while Broso usually extracted the RNA from intact EBs.

Gene	Group	Mutant 377 (Day 12) FC from WT	P value
Nkx2.5	Early Cardiac	2.11 (0.95-3.01)	0.0684
MYH6	Late Cardiac	1.70 (0.75-3.10)	0.2076
MYH7	Late Cardiac	2.10 (0.39-3.05)	0.1824
MYL2	Late Cardiac	2.44 (0.28-2.76)	0.1755

Table 4 Results of the analysis on cardiac markers at day 12 of differentiations. *Data are based on 8 independent differentiations; the non-parametric one-sample Wilcoxon signed –rank test analysis has been employed and no statistically significantly difference in the expression of the late cardiac markers was observed. The p value obtained for Nkx2.5 (p value <0.10), however, indicates a trend of modulation of this early cardiac gene; but a fold change with a value less of 2 is considered not biologically significant (Hu et al., 2006).*

Striatin-interacting proteins

The expression levels of some genes coding for Striatin-interacting proteins as protein phosphatase 2 scaffold subunit A alpha (PPP2R1A), β-catenin (CTNNB1) and Connexin 43 (GJA1) were also analyzed. Medians of fold changes with relative interquartile range for each gene at day 12 of differentiation are reported in Table 5. It is interesting to notice that Beta Catenin, a well known Striatin-interacting protein (Franke et al., 2015, Oxford et al., 2014, Meurs et al., 2013), appeared down-modulated, but a fold change with a value less than 2 which is considered not biologically significant (Hu et al., 2006).

Additionally, in this work, mutants seemed to express a higher level of HCN4. This result is in line with the higher frequency of spontaneous AP firing in mutant vs WT (see below). A further trend in upregulation was also observed in RyR2 and SERCA2A expression, although a fold change with a value less than 2 is usually considered not biologically significant (Table 5) (Hu et al., 2006).

Gene	Group	Mutant 377 (Day 12) FC from WT	P value
HCN1	Ion channels	1.48 (0.91-2.52)	0.0687
HCN4	Ion channels	1.92 (1.05-2.34)	0.0499
KCNJ2	Ion channels	1.21 (0.81-1.44)	0.2076
CACNA1C	Ion channels	1.00 (0.69-1.4)	0.7532
SCN5A	Ion channels	1.47 (0.92-2.41)	0.1730
RyR2	Ion channels	2.40 (0.97-3.07)	0.0687
ATP2A2 (SERCA2A)	Ion channels	1.37 (0.91-1.66)	0.0687
CTNNB1 (ß-CATENIN)	Striatin-interacting	1.25 (1.03-1.46)	0.0328
GJA1 (CX43)	Striatin-interacting	1.16 (0.83-1.41)	0.3980
PPP2R1A	Striatin-interacting	1 (0.81-1.82)	0.6741
BMP10	negatively regulated by Nkx2.5	1.08 (0.77-1.17)	0.9163
RSPO3	positively regulated by Nkx2.5	1.17 (0.97-1.38)	0.1730
TGFBR3	positively regulated by Nkx2.5	1.08 (0.85-1.46)	0.5282

Table 5. Results of the analysis of ion channels genes and Striatin-interacting protein at day 12 of differentiation. *Data are based on eight independent differentiations. For Striatin-interacting proteins, the reported genes were considered based on literature data and focused on possible cardiac involvement of Strn. An increased expression for CTNNB1 (p=0.0328) and If channel gene HCN4 (p=0.0499) at day 12 was apparent in the Striatin-mutant, while the p-value obtained for HCN1, RyR2 and ATP2A2 indicated a trend of modulations.*

The non-parametric one-sample Wilcoxon signed –rank test pointed out a significant difference in CTNNB1 expression at day 12 (p=0.0328) and an increased expression for I*f* channel gene HCN4, was apparent in the Striatin-mutant, (p=0.0499).

15. *Functional characterization of Strn-mutant*

15.1 Video Tracker analysis

A video analysis of beating areas has been performed to evaluate possible differences in the contractile activity of mutant- versus WT- derived beaters. This analysis has been performed on the recorded video of beating area at day 11-12 of differentiation by Dr. Lorenzo Fassina at the University of Pavia, following the method described in L. Fassina et al, 2011 and using the Video Spot Tracker (VST) program available online (http://www.cs.unc.edu/~nanowork/cismm/download/spottracker/video_spot_tracker.html).

In particular, after manually defining a 30 spots or marker for each beating area, the program automatically followed and registered the spatial coordinates x, y during time for every marker. After plotting the displacement of x for WT (Fig. 14A) and mutants (Fig. 14B) marker it has been possible to see that the mutant loss some beats. As a consequence, a reduction of the contraction frequency and a lack of rhythmicity (arrows in red) were observed in mutants compared to the WT.

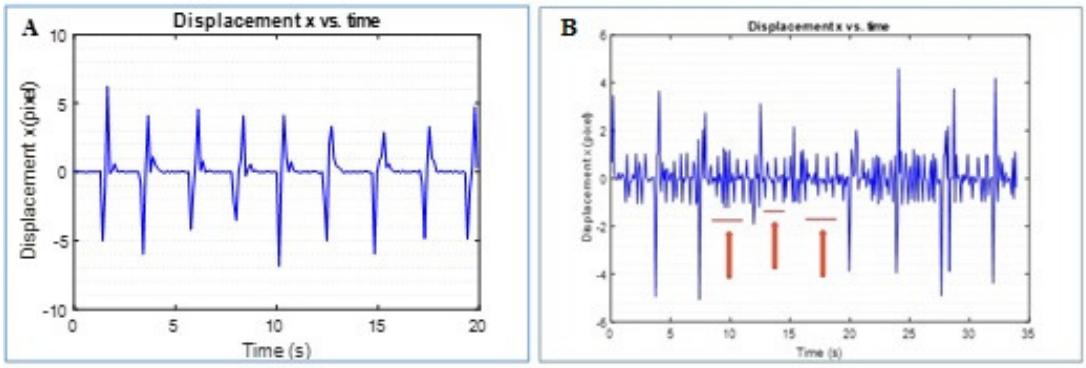

Fig. 14 Displacement of the spatial coordinates x. *The displacement of x for a wild type marker (A) and a mutant marker (B) shows that the WT have a regular contraction frequency, while the mutant loss some beats indicated from the arrows in red, and this induces a reduction of the contraction frequency and a lack of rhythmicity.*

Specifically, although a dysregulated contraction performance was observed in wild type as well as in mutant EBs, the incidence of this behavior was significantly higher in Strn-mutants 72.2% (n=19) when compared to WT 22.2% (n=19) suggesting an abnormal contraction activity associated with the lack of Striatin (Fig. 15)

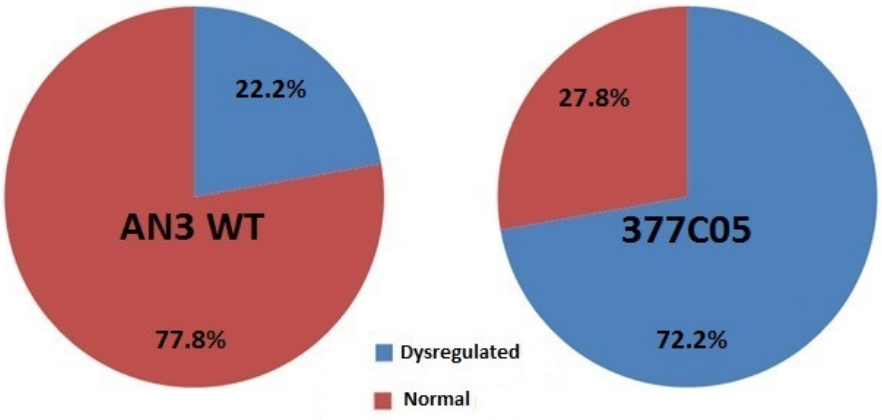

Fig. 15 Dysregulated contraction performance. *Evaluation of dysregulated contraction behavior showed an increased presence of loss of beats in mutant respect as compared with wild type EBs. The incidence of dysregulated contraction was higher in Strn-mutants compared to WT.*

Of note, in opposition to what reported by Broso F. (Broso F., Tesi di Laurea, 2014) we observed a significant reduction of the contraction frequency (p value < 0.0001) in the 377C05 mutant (mean 0.38Hz) respect to the AN3 wild type (mean 0.62 Hz) at day 12 (Fig. 16). The discrepancy with our preliminary data can be explained considering that in this version of the work new experiments were performed using CMs obtained from mESCs cultured on a MEF feeder layer. In addition, in the present version of the analysis only beats associated with a significant pixel displacement were counted (see Methods).

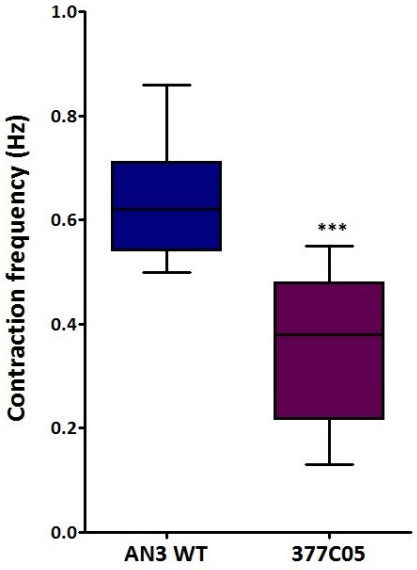

Fig. 16 Evaluation of the contraction areas. *The frequency of the contraction of beating areas has been assessed by video analysis (according to L. Fassina et al 2011). Results are expressed as average with 95% confidence intervals (***p < 0.0001; non-parametric Mann-Whitney test).*

The videos of two markers were online:

AN3 WT: https://gemex.eurac.edu/downloads/VideoTrackerAnalysis/AN3WT.avi

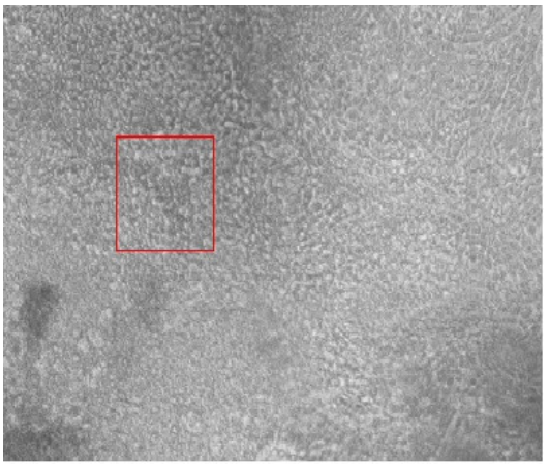

377C05:https://gemex.eurac.edu/downloads/VideoTrackerAnalysis/377C05.avi

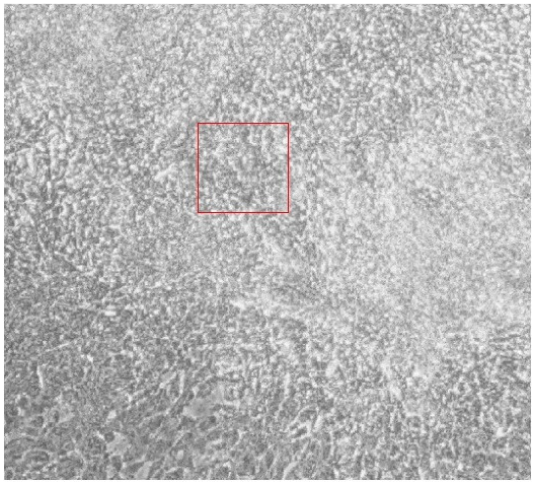

15.2 Electrophysiological recordings

Electrophysiological recordings have been performed on micro-dissected beating areas (from D12 to D15). Action potentials (APs) generated by spontaneously active cells were measured by using the patch-clamp technique (current-clamp mode) (Fig. 17A).
The frequency distribution of APs was skewed towards higher values in Strn-mutant EBs with respect to the distribution displayed by the wild-type ones. Mean frequency values obtained were 0.88 ± 0.06 Hz and 1.71 ± 0.17 Hz for WT (n=25) and mutants (n=22), respectively (Fig. 17B; $p<0.001$).

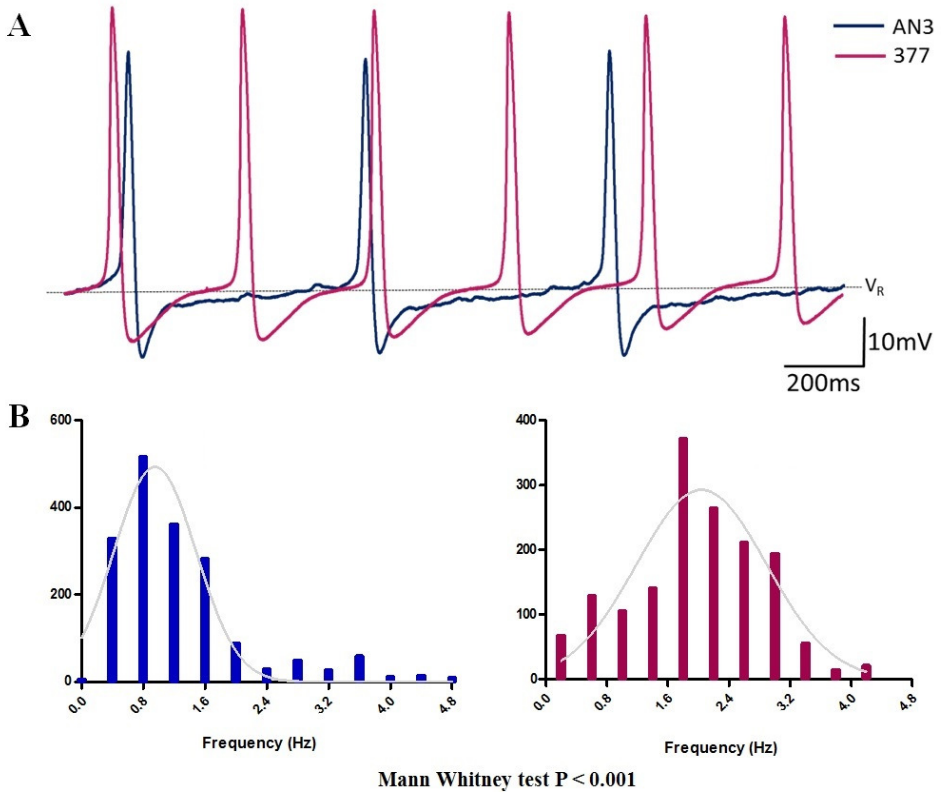

Fig. 17 Spontaneous AP firing pattern. *(A) Representative traces of APs generated by active cells from micro-dissected beating area (from D12 to D15) of WT (blue line) and Strn mutant EBs (purple line); (B) Frequency distribution histograms show significant differences in the mean frequency values obtained from 25 cells WT (0.88 ± 0.06 Hz-blue) and 22 cells of Strn-mutant (1.71 ± 0.17 Hz-purple) preparations. The comparisons between WT and 377 were made by a non-parametric Mann-Whitney test electing a significance level of 0.05*

Moreover, Strn-mutant EBs showed, on average, a remarkable reduction in AP duration (APD) evaluated during the early (APD_{20}, WT: 99.4±29.5 ms; 377C05: 74.7±23.0 ms), middle (APD_{60}, WT: 128.8±44.0 ms; 377C05: 93.6±29.7 ms) and late (APD_{90}, WT: 146.5±56.6 ms; 377C05: 104.9±32.0 ms) phases of repolarization. Conversely, no differences were observed for the other AP parameters, as the action potential amplitude (APA, WT: 60.2±21.4 mV; 377C05: 60.5±18.4 mV), the upstroke (peak, WT: 19.4±8.8 mV; 377C05: 19.9±7.4 mV), the maximum diastolic potential (MDP, WT: -40.9±15.2 mV; 377C05: -40.64±14.8 mV) and the takeoff potential (TOP, WT: -31.9±13.1 mV; 377C05: -31.78±12.1 mV)(Fig. 18).

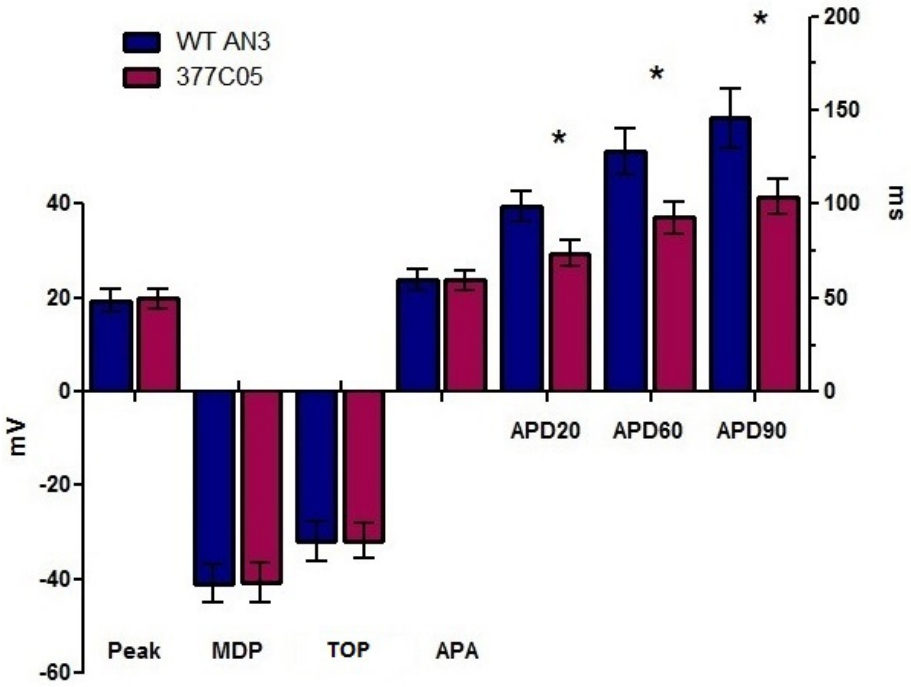

Fig. 18 Action Potential Parameters. *Different AP parameters were evaluated in order to assess the effect of the Strn-mutation. The bar-chart plot shows the mean values for the upstroke, maximum diastolic potential, TOP, action potential amplitude (APA) and action potential duration (APD); evaluated at three different times of the repolarization phase obtained from WT (n=14) and 377 (n=13) preparations. A significant reduction of the APD values, despite the time evaluated, was observed in Strn-mutants with respect to the WT. Values are expressed as mean ± SEM; * p<0.05 Mann-Whitney test.*

Figure 19 displays the mean values of inter-event-interval obtained for WT (0.21 ± 0.006; n=19) and Strn mutants (0.24 ± 0.013; n=19). These data suggest that the Strn-mutant cardiomyocytes might exhibit irregular firing compared to the WT, in accordance with the trend towards an increase in the coefficient of variation of IEI (CV-IEI) observed in the Strn-mutant recordings.

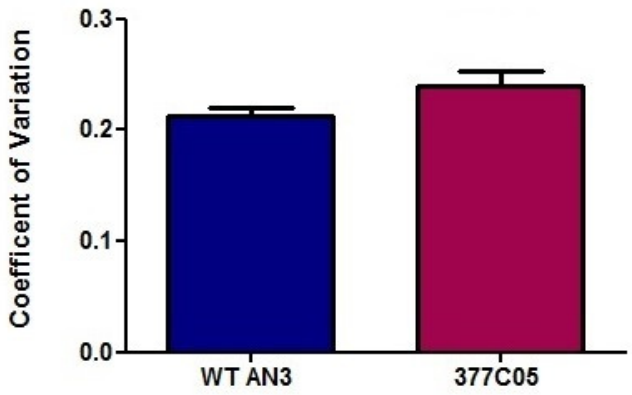

Fig. 19 Coefficient of variation of the inter-event-interval (CV-IEI). *The inter-event-interval (IEI) is the elapsed time between the peak of an AP to the peak of the next one. The bar chart graph shows the comparisons of the ratio between the standard deviation of the IEI and the mean value of the IEI. Non-parametric Mann-Whitney test that shows a trend (p=0.0749)*

Sometimes during the electrophysiology recording of spontaneous action potentials, micro-dissected beating areas displayed an extreme arrhythmic behavior characterized by the presence of bursts of APs interrupted by no-activity periods (Fig. 20, representative traces).

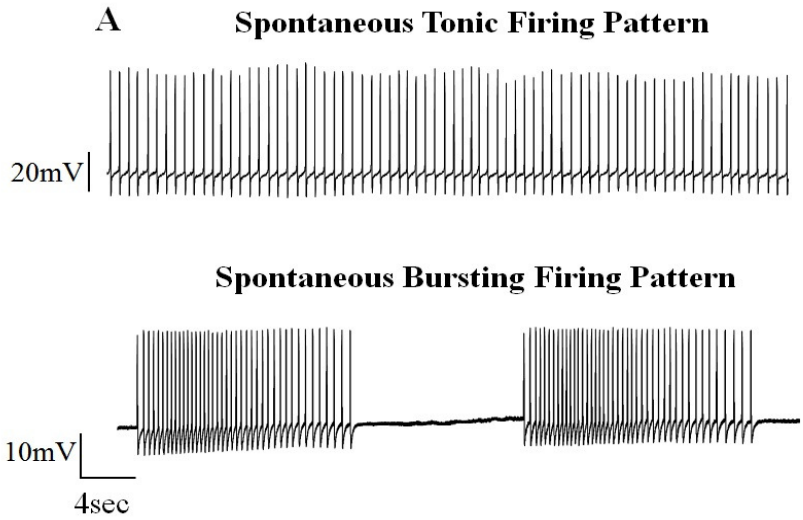

Fig. 20 Spontaneous bursting activity of beating areas. *Representative traces of tonic firing pattern, with a regular activity (up) and bursting firing pattern where bursts of APs were interrupted by no-activity periods (down). These behaviors were observed in our preparations preparation, in both cells lines.*

This activity was observed in wild type as well as in mutant preparations. However, the incidence of this behavior was higher in Strn-mutants 32% (n=22) when compared to WT 14% (n=29), suggesting an abnormal likelihood in the generation of arrhythmic activity associated with the lack of Striatin (Fig. 21).

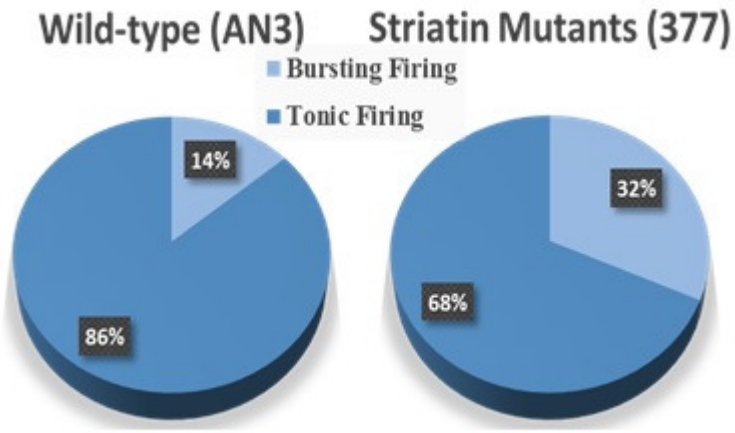

Fig. 21 Evaluation of bursting spontaneous firing. *Bursting firing pattern, where bursts of APs were interrupted by no-activity periods are present in 32% of EBs mutant respect the to14% in wild type EBs*

15.3 Calcium imaging

In order to examine the calcium-induced calcium release process (i.e. the coupling between an action potential and its evoked calcium release from the SR we performed, in the same beating area, calcium imaging acquisitions using a fluorescent dye (i.e. Fluo-4) coupled to spontaneous APs recordings using the patch-clamp technique (i.e. current-clamp mode, whole-cell configuration). Figure 22 shows representative traces of these recordings obtained for WT (Fig. 22A) and for Strn-mutant (Fig. 22B and C) preparations. No differences between groups were observed on the capability of an AP to evoke a calcium transient, being apparent that each AP was associated with a calcium transient in the recordings coming from both groups. However, a delay in the appearance of calcium peak was occasionally present in the mutant (Fig. 22C).

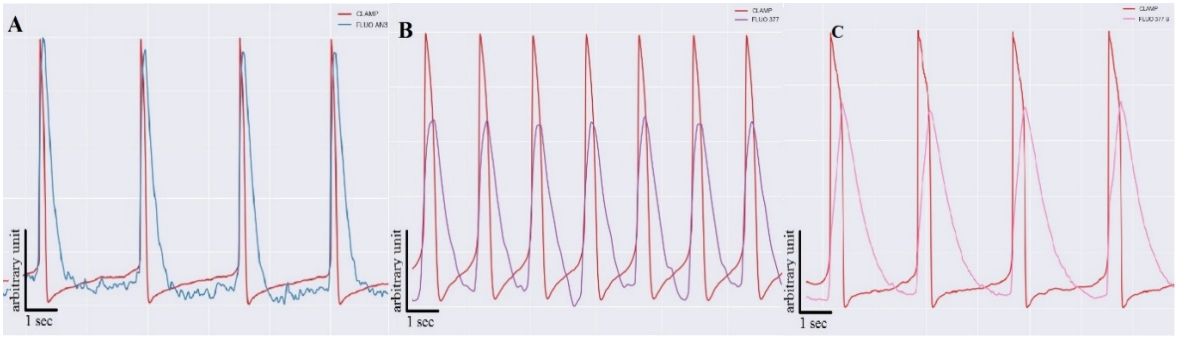

Fig. 22 Calcium-induced calcium release traces. *Representative traces of calcium imaging acquisitions (blue line AN3 and purple and pink line 377C05) and electrophysiological recordings (Red line) simultaneously recorded inside the same beating area. No differences, between our experimental groups, have been observed. In fact, every AP was able to generate a calcium spike. However, figure C shows that sometimes the mutant has a delay in the calcium spike.*

Focusing on the dynamics of calcium release, the time between the peak of calcium transient and the peak of AP was measured. Plotting this delay for both cells lines, only a max peak was observed in wild type line approximately after 150 ms, while in the mutant, beyond the maximum peak at the same delay, two other peaks were present at more high delays; about after 300 and 450 milliseconds (Fig. 23).

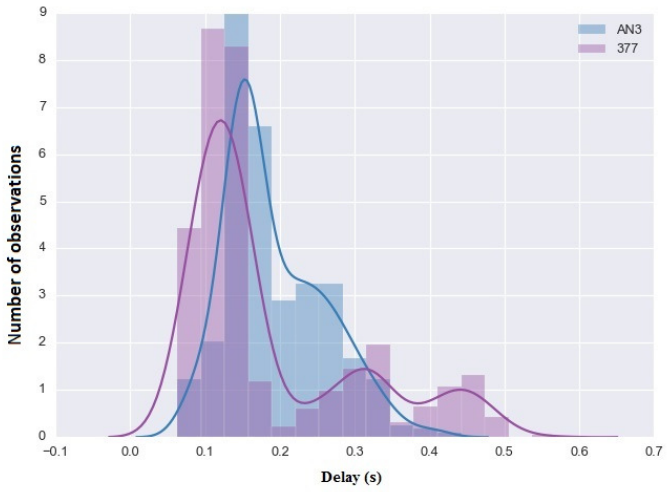

Fig. 23 Calcium dynamics. *The delay between the peak of calcium transient and the peak of AP shows that one max peak was present in wild type approximately after 150 milliseconds (blue line). In the mutant, one peak was present at the same delay (after 150 milliseconds), but two other peaks appear after 300 and 450 milliseconds.*

To evaluate the amount of Ca^{2+} released by the two cellular lines we measured the peak of calcium fluorescence released after the spontaneous AP. The mean fluorescence, calculated at the peak of the calcium transient, was about twice greater in wild-type than the mutant; indicating a significant reduction of calcium released from mutant cell line (3.24 in WT and 1.33 in 377C05, p value < 0.001; Fig. 24A).

Even if the amount of calcium is reduced in the cardiomyocytes obtained from mutant, we did not observe any difference in the variability of calcium release between the two groups (0.03±0.006 in WT and 0.03±0.007 in mutant, Fig. 24B), expressed as the ratio between the standard deviation of the calcium peaks and the mean value of the peaks ($CV_{peak\text{-}Ca2+}$= $SD_{peak\text{-}Ca2+}$ / $MEAN_{peak\text{-}Ca2+}$).

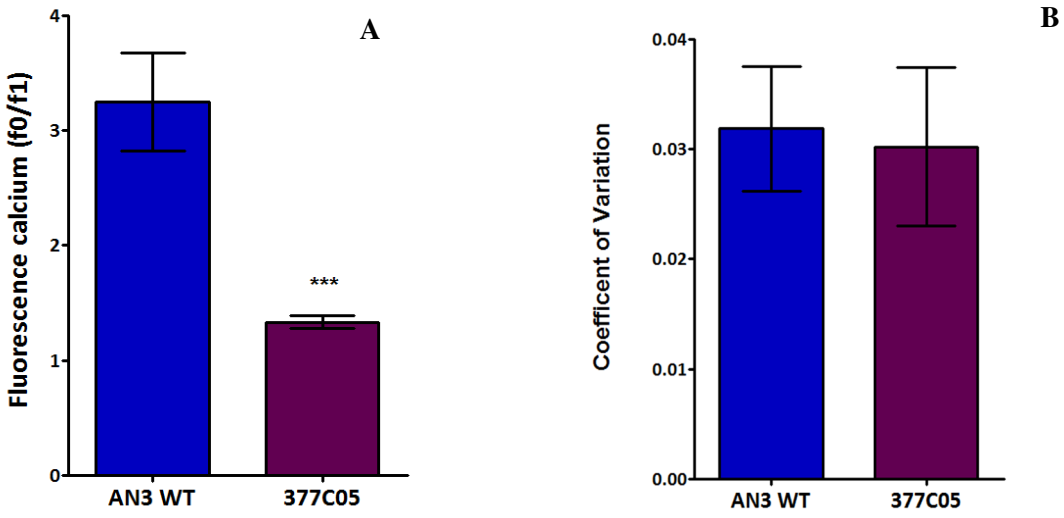

Fig. 24. Amount of calcium. *The amount (A) and the variability of release (B) of calcium have been assessed by the fluorescence. The mean fluorescence for wild type was about twice greater than the mutant (p < 0.0001; non-parametric Mann-Whitney test). However, the variability of release of calcium was similar in the two groups. The variability was calculated as the ratio between the standard deviation of the calcium peaks and the mean value of the peaks.*

The recovering kinetics for the calcium were estimated from AN3 WT and 377C05 mutant traces. On average, no difference was found at the 20% (Recovery 20%, WT: 170±5 ms; 377C05: 160±4 ms), and the 60% (Recovery 60%, WT: 430±1 ms; 377C05: 440±1 ms) of reuptake (Fig. 25).

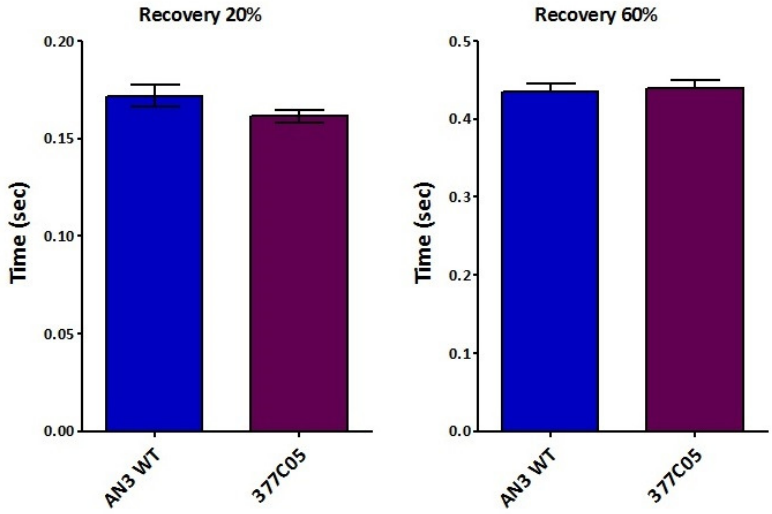

Fig. 25 Recovery of calcium. *The reuptake of calcium was evaluated in order to assess the effect the Strn-mutation. The bar graph shows the mean values of two different times of recovery phases obtained from WT (n=333 spikes) and 377 (n=642 spikes). No difference was observed between groups. Values are expressed in mean ± SEM.*

16. *Immunofluorescence*

In order to evaluate the organization of the sarcomere structure in differentiated cardiomyocytes (day 20), we analyzed by immunofluorescence the pattern of configuration of the sarcomeric protein troponin T.

On wild-type cardiomyocytes, the troponin T generally displayed the sarcomere-specific striated pattern (Fig. 26A), while on cardiomyocytes obtained from Strn- mutants this pattern revealed disorganized and disoriented sarcomeres with absence of the typical striated configuration for the

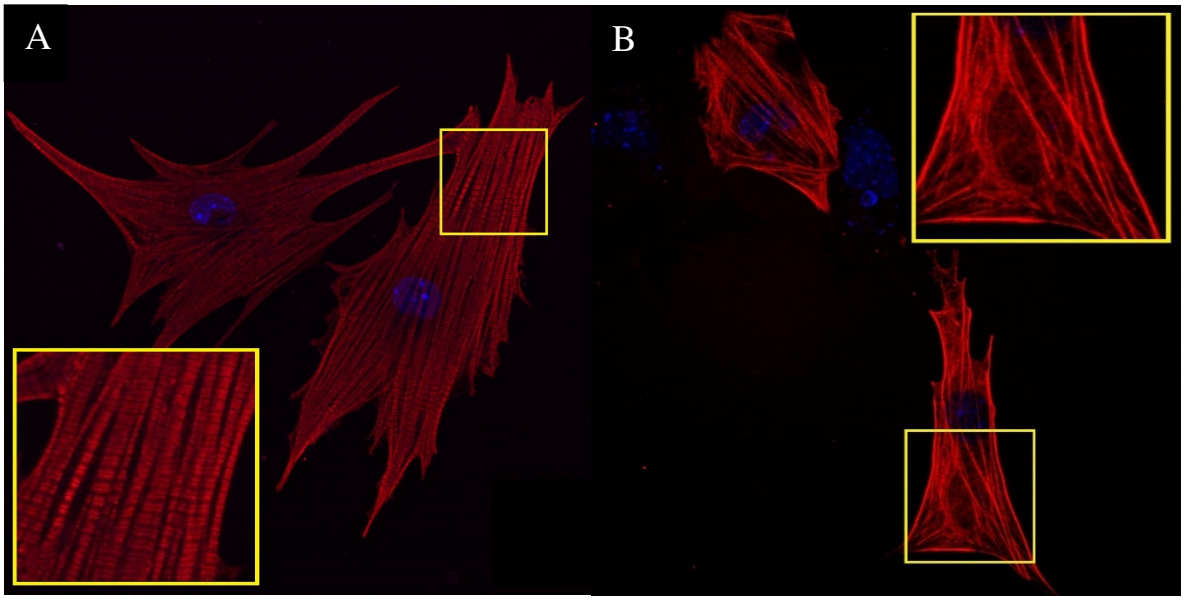

Fig. 26 Sarcomere structure organization. *Localization of cardiac troponin T (red fluorescence) in wild type cardiomyocytes (A) and Strn-mutant lines (B) at day 20 of differentiation. The nuclei were colored with DAPI (blue). For each line, about 100 cells were analyzed. The insert shows the details of the structure; The mutant revealed disorganized and disoriented sarcomeres with absence of the typical striated configuration for the troponin T protein*

troponin T protein (Fig. 26B).

A quantification of this structural defect showed a significant difference on its occurrence when evaluated in WT or Strn-mutant cardiomyocytes *in vitro* (Fig. 27). The percentage of cardiomyocytes displaying a correct sarcomere organization was 77 ± 7% and 51 ± 8% for WT (n=84) and Strn-mutants (n=102), respectively (P value = 0.0129, non- parametric Mann-Whitney test).

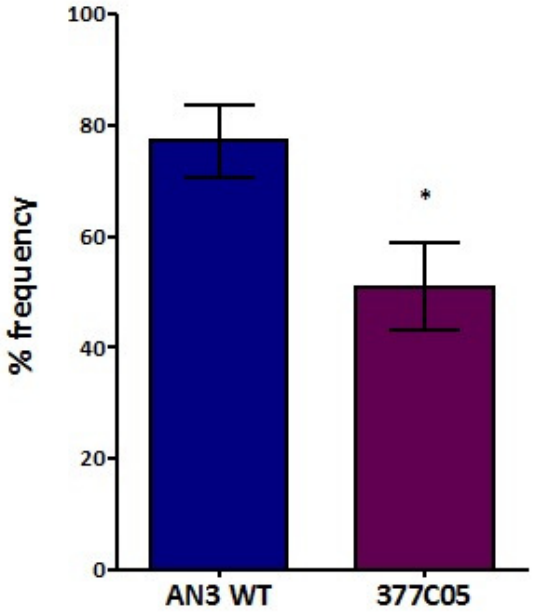

Fig. 27 Frequency of cardiomyocytes with correct sarcomeric organization. *Immunofluorescence was performed on dissociated-EBs. The frequency was calculated counting the ratio between the cells with a correct striated pattern and the number of nuclei.*

Discussion

Mouse embryonic stem cells (mESCs) have recently been suggested as a good tool for genetic screens (Elling et al., 2011). Possessing one copy of each gene, they facilitate the generation of loss-of-function mutants that represent a powerful tool to investigate the role of new target genes. mESCs maintain haploidy and stable growth during extensive *in vitro* culture, express the pluripotent markers and possess the ability to differentiate into the three germ layers *in vitro* and *in vivo* (Shuai and Zhou, 2014). However, mESCs have not been used so far as a model to study the differentiation process *in vitro*.

Recently, the product of the STRN gene was associated with a reduction in diastolic diameters and contractility and disruption of myofibryllar organization in Drosophila (van der Harst et al., 2016). Some cardiovascular diseases have been associated to the mutation of the Striatin gene, as arrythmogenic right ventricular cardiomyopathy (ARVC) and dilated cardiomyopathy in dogs (Meurs et al., 2010, Meurs et al., 2013); Additionally, in a GWAS in humans, the locus of the Striatin has been associated with changes in the QRS complex duration in turns associated to ventricular conduction defects (Sotoodehnia et al., 2010).

In the present work, we confirm that Striatin-mutation can lead to important alterations of the cardiomyocyte function by using haploid mouse stem cells mutated in the STRN gene.

Importantly, this thesis is part of a wider project conducted in our laboratory. The haploid mESC wild type (WT AN3) and the mutant cell line (377C05) used in the present work were kindly provided by Prof. Joseph Penninger group (IMBA, Vienna); and as outlined in the introduction, preliminary experiments were performed by Piubelli C. and Broso F. (Broso F., Tesi di Laurea, 2014).

In this report, we used Striatin-mutant cardiomyocytes derived from haploid mESCs to evaluate functional alteration associated with the absence of this scaffold protein using two different independent approaches. The first one was the use of video tracker algorithm to measure contraction, while the second one was an electrophysiology approach in order to assess the AP generation capacity of the cells and the AP features.

The video analysis results showed that the frequency of contraction, at day 12, was lower in the mutant 377C05 with respect to WT. Likewise, this analysis allows us to observe that 72% of beating areas obtained from the mutant manifested a loss of contractions, and this induces a reduction of the

contraction frequency and a lack of rhythmicity. The apparent contrast to what reported by Broso F. (Broso F., Tesi di Laurea, 2014) can be explained by considering that here an algorithm was used in order to filter high frequency displacement corresponding to beating artifacts.

These results, therefore, might suggest that one or more steps on the EC-coupling process could be compromised as a consequence of the Striatin-mutation.

Unexpectedly, when the spontaneous action potential firing was evaluated by electrophysiological recordings, we observed that AP frequency was higher in Strn-mutant EBs than in wild-type. In accordance with previous findings demonstrating that AP frequency is associated with the hyperpolarization-activated pacemaker current, *If* (DiFrancesco, 2010), we detected an increase in the mRNA expression of the hyperpolarization-activated cyclic nucleotide-gated channel 4 (HCN4) (Seifert et al., 1999). I*f*, in turns, regulates the duration of the diastolic depolarization phase and thus the firing frequency of the action potentials (DiFrancesco, 2006). Additionally, a reduction in the duration of the APs and a trend of increase in the coefficient of variation of the inter-AP-interval (inter-event-interval) were also observed in mutant CMs respect to controls, indicating an important effect of Striatin-mutation on cell electrophysiology. The changes observed during repolarization might suggest the activation of homeostatic compensatory mechanisms on the currents mediating these processes (i.e. funny, potassium and calcium currents). Some EBs, in plus, displayed an extreme arrhythmic behavior being apparent by the presence of bursts of APs interrupted by no-activity periods. This activity was observed in WT as well as in mutant EBs, but the incidence of this behavior was higher in Strn-mutants, suggesting an abnormal likelihood in the generation of arrhythmic activity associated with the lack of Striatin

Further electrophysiological characterization is needed in order to determine the role of putative alterations of specific ionic conductances in the observed differences between WT and mutants.

Importantly, a decrease in contraction frequency, accompanied by an increase of AP firing rate seems to indicate that in contrast to the WT, there is not a correlation 1:1 between an action potential generation and a muscle contraction in Strn-mutant derived cardiomyocytes.

This conflicting results prompted us to investigate the presence of a possible problem at the level of excitation-contraction coupling. First, we evaluated the coordination between the action potential generation and the release of Ca^{2+} from the sarcoplasmic reticulum (SR). Simultaneous recordings of

calcium signals and spontaneous firing activity did not show decoupling between the AP generation and the induced calcium release. Indeed, every AP spike was associated with a calcium spike in both, WT and mutant preparations. However, even if each action potential evoked a calcium transient, the amount of calcium and the dynamics of the calcium release displayed some differences associated to the Striatin-mutation. In fact, the mean amplitude of Ca^{2+} transients after a spontaneous AP was about twice lower in the mutants. In addition, the time delay distribution of the calcium transient peak with respect to the corresponding AP peak displayed a distribution bias for higher values in the Striatin-mutants as compared with WT cardiomyocytes. This indicates that in the mutants, the calcium release was not only smaller in average but also its release was less efficiently coupled to the AP spike.

Second, we analyzed the structural organization of the contractile machinery of the *in vitro* differentiated cardiomyocytes coming from both experimental groups. To investigate the sarcomere structure in differentiated cardiomyocytes, we used the protocol suggest by Rebuzzini and colleagues (Rebuzzini et al., 2015). The immunofluorescence showed that 49 % of cardiomyocytes obtained from Strn- mutants presented disorganized and disoriented sarcomeres with absence of the striated configuration for troponin T. These data are in complete agreement with the result showed by Van der Harst (van der Harst et al., 2016) and colleagues, where heart-specific RNAi knockdown for Cka/Striatin in Drosophila melanogaster induced myofibrillar disarrangement with myofibrils oriented in a disorganized manner.

Guzzo and colleagues (Guzzo, 2005), also demonstrated that the complex of Striatin and other component of Striatin family, called STRIPAK interacts with the myofibrils, regulating the structural arrangement of the E-C coupling apparatus in cardiomyocytes

In the same way, Meurs and colleagues (Meurs et al., 2013) demonstrated that the Striatin-mutation could result in alteration of desmosome integrity in boxer dogs with ARVC. Furthermore, in this article for the first time, ß-catenin and Striatin are showed to be co-localized into the endoplasmic reticulum.

β-catenin is not only a component of the adherence junctions, but is also the player of the Wnt canonical pathway, which is involved in cardiomyogenic differentiation, by orchestrating the complex organization and dynamics of the cardiac cell cytoskeleton (Chen et al., 2008). Thus, we can speculate that the involvement of this pathway might explain the difference revealed in the expression of the early cardiac transcription factor Nkx2.5 and the detected reduced number and dimension of

beating areas in the mutant 377C05 at day 12 of differentiation, being in line with the altered expression of the ß-catenin also observed in our experimental data.

We tested, in plus, whether the mutant displayed some differences in the pluripotency and cardiac gene expression when compared to the WT during the *in vitro* differentiation. As expected, a decrease in the pluripotency gene was observed in both groups, being also similar in their proportions; and the cardiac genes should progressively appear according to the differentiation stage.

The entirety of our data indicates that the apparent difference between WT and mutant at the level of contraction and APs firing could be explained by a concurrency of an altered induced calcium release, as shown in the calcium imaging experiments, and a structural dysregulation of the contractile machinery due to the Striatin lack., as demonstrated through confocal analysis.

In conclusion, possibly as a result of its scaffolding properties (Gaillard et al., 2001), Striatin, when knocked out, does not induce changes at the level of cardiac gene expression, but determines significant changes in cardiomyocyte electrophysiological properties, a dysregulation of the excitation-contraction coupling and a disorganization of the sarcomere machinery.

Taken together our results confirm that Striatin is a possible new target in cardiovascular disease.

Future Work

The functional characterisation will be performed in order to determine the role of putative alterations of specific ionic conductances in the observed differences between WT and mutants; in particular additional electrophysiological experiments will be done to investigate the current *If* and the potassium channel, respectively responsible for the diastolic depolarization phase and the duration of action potential.

Moreover some interesting pathways highligheted by the molecular characterisation will be explored, like the Wnt-Beta catenin pathway.

Finally, to confirm our data by *in vivo* results, a collaboration with the group of Prof. Bodmer (Sanford-Burnham Medical Research Institute) will be started to evaluate Strn mutants in Drosophila pupae.

ACKNOWLEDGEMENTS

I would like to express my special appreciation and thanks to my advisor Professor Dr. Donatella Stilli, for her work as supervisor and mentor during my Ph. D program.

I wish to express my gratitude at the Group Leader of the cardiovascular medicine, Dr. Alessandra Rossini for having encouraged my research and for allowing me to grow as a research scientist.

I would also like to thank all members of EURAC Research in Bozen for the great availability and affection, the help in writing of this thesis and for continuous encouragement during these PhD years.

Special thanks to Dr. Chiara Piubelli and Francesca Broso, who have characterized the haploid stem cell lines; especially thank Francesca Broso for the figure 8 which belong to her Master's thesis (Broso F., Tesi di Laurea, 2014). Thanks to Dr. Marcelo Rosato Siri for helping me to complete the work of this thesis, mostly for many hours spent to do the electrophysiology experiments. Dr. Yuri D´Elia for the production in Linux of the home-made software ClampMatic and CalciumStat.

I would like to express my special appreciation to Dr. Andrea Barbuti and his staff (Giulia, Patrizia and Mattia) of The PaceLab at the University of Milan for professional advice and support that have helped to improve this project and to Dr. Lorenzo Fassina of the Department of Electrical, Computer and Biomedical Engineering, University of Pavia for all video analysis.

Thanks to Viviana, Cristina, Benedetta M, Christa, Julia, Alessandra P., Marianna, Damia, Antonia, for all the happy moments we spent together, you all contributed to render this experience unforgettable. Cristina B. for every your embrace in times of despair and Claudia for your “mammy´s words” always appreciated.

I also wish to thank:

My family, words cannot express how grateful I am to your unconditional support in all these years; My parents which have given up many things to make me stay at Bozen; you have cherished with me every great moment and you have supported me whenever I needed it. You are the most basic source of my life energy resides. I would also like to thank my brother who supported me in every way, and encouraged me to reach my goal and to overcome it.

I must express my deep gratitude to Serena, "la mia Cicci", for sharing with me this crazy experience, called PhD. We have never stopped to go crazy together.

I would like to thanks the crazy part of my life, my second family, Valentina and Enrica, “Sore e Gi”, because you have supported me, encouraged, incited and believed in me at all times and in all fight.

At the end I would like express my appreciation to my beloved boyfriends Luca who spent sleepless nights with me and was always my support in the moments when there was no one to do it. You're my lifeline, always!

Bibliography

BAILLAT, G., MOQRICH, A., CASTETS, F., BAUDE, A., BAILLY, Y., BENMERAH, A. & MONNERON, A. 2001. Molecular cloning and characterization of phocein, a protein found from the Golgi complex to dendritic spines. *Mol Biol Cell,* 12**,** 663-73.

BARTOLI, M., MONNERON, A. & LADANT, D. 1998. Interaction of calmodulin with striatin, a WD-repeat protein present in neuronal dendritic spines. *J Biol Chem,* 273**,** 22248-53.

BARUSCOTTI, M., BIANCO, E., BUCCHI, A. & DIFRANCESCO, D. 2016. Current understanding of the pathophysiological mechanisms responsible for inappropriate sinus tachycardia: role of the If "funny" current. *J Interv Card Electrophysiol,* 46**,** 19-28.

BEHFAR, A., ZINGMAN, L. V., HODGSON, D. M., RAUZIER, J. M., KANE, G. C., TERZIC, A. & PUCEAT, M. 2002. Stem cell differentiation requires a paracrine pathway in the heart. *FASEB J,* 16**,** 1558-66.

BERS, D. M. 2002. Cardiac excitation-contraction coupling. *Nature,* 415**,** 198-205.

BETTIOL, E., CLEMENT, S., KRAUSE, K. H. & JACONI, M. E. 2006. Embryonic and adult stem cell-derived cardiomyocytes: lessons from in vitro models. *Rev Physiol Biochem Pharmacol,* 157**,** 1-30.

BILIC, J. & IZPISUA BELMONTE, J. C. 2012. Concise review: Induced pluripotent stem cells versus embryonic stem cells: close enough or yet too far apart? *Stem Cells,* 30**,** 33-41.

BOHELER, K. R. 2003. ES cell differentiation to the cardiac lineage. *Methods Enzymol,* 365**,** 228-41.

BOHELER, K. R., CZYZ, J., TWEEDIE, D., YANG, H. T., ANISIMOV, S. V. & WOBUS, A. M. 2002. Differentiation of pluripotent embryonic stem cells into cardiomyocytes. *Circ Res,* 91**,** 189-201.

BRAAM, S. R., TERTOOLEN, L., VAN DE STOLPE, A., MEYER, T., PASSIER, R. & MUMMERY, C. L. 2010. Prediction of drug-induced cardiotoxicity using human embryonic stem cell-derived cardiomyocytes. *Stem Cell Res,* 4**,** 107-16.

BRATT-LEAL, A. M., CARPENEDO, R. L. & MCDEVITT, T. C. 2009. Engineering the embryoid body microenvironment to direct embryonic stem cell differentiation. *Biotechnol Prog,* 25**,** 43-51.

BRITO-MARTINS, M., HARDING, S. E. & ALI, N. N. 2008. beta(1)- and beta(2)-adrenoceptor responses in cardiomyocytes derived from human embryonic stem cells: comparison with failing and non-failing adult human heart. *Br J Pharmacol,* 153**,** 751-9.

BROWN, C. O., 3RD, CHI, X., GARCIA-GRAS, E., SHIRAI, M., FENG, X. H. & SCHWARTZ, R. J. 2004. The cardiac determination factor, Nkx2-5, is activated by mutual cofactors GATA-4 and Smad1/4 via a novel upstream enhancer. *J Biol Chem,* 279**,** 10659-69.

BROWN, H., DIFRANCESCO, D. & NOBLE, S. 1979. Cardiac pacemaker oscillation and its modulation by autonomic transmitters. *Journal of Experimental Biology,* 81**,** 175-204.

BROSO, F. & PIUBELLI, C. 2014 A MOUSE MODEL OF HAPLOID EMBRYONIC STEM CELLS TO STUDY THE ROLE OF STRIATIN IN CARDIOMYOGENIC DIFFERENTIATION. Master Thesis, University of Trento

BRYJA, V., BONILLA, S. & ARENAS, E. 2006. Derivation of mouse embryonic stem cells. *Nat Protoc,* 1**,** 2082-7.

CAMBIER, L., PLATE, M., SUCOV, H. M. & PASHMFOROUSH, M. 2014. Nkx2-5 regulates cardiac growth through modulation of Wnt signaling by R-spondin3. *Development,* 141**,** 2959-71.

CASPI, O., ITZHAKI, I., KEHAT, I., GEPSTEIN, A., ARBEL, G., HUBER, I., SATIN, J. & GEPSTEIN, L. 2009. In vitro electrophysiological drug testing using human embryonic stem cell derived cardiomyocytes. *Stem Cells Dev,* 18**,** 161-72.

CASTETS, F., BARTOLI, M., BARNIER, J. V., BAILLAT, G., SALIN, P., MOQRICH, A., BOURGEOIS, J. P., DENIZOT, F., ROUGON, G., CALOTHY, G. & MONNERON, A. 1996. A novel calmodulin-binding protein, belonging to the WD-repeat family, is localized in dendrites of a subset of CNS neurons. *J Cell Biol,* 134**,** 1051-62.

CASTETS, F., RAKITINA, T., GAILLARD, S., MOQRICH, A., MATTEI, M. G. & MONNERON, A. 2000. Zinedin, SG2NA, and striatin are calmodulin-binding, WD repeat proteins principally expressed in the brain. *J Biol Chem,* 275**,** 19970-7.

CHEN, Y., STUMP, R. J., LOVICU, F. J., SHIMONO, A. & MCAVOY, J. W. 2008. Wnt signaling is required for organization of the lens fiber cell cytoskeleton and development of lens three-dimensional architecture. *Dev Biol,* 324**,** 161-76.

COWAN, C. A., KLIMANSKAYA, I., MCMAHON, J., ATIENZA, J., WITMYER, J., ZUCKER, J. P., WANG, S., MORTON, C. C., MCMAHON, A. P., POWERS, D. & MELTON, D. A. 2004. Derivation of embryonic stem-cell lines from human blastocysts. *N Engl J Med,* 350**,** 1353-6.

CZECHANSKI, A., BYERS, C., GREENSTEIN, I., SCHRODE, N., DONAHUE, L. R., HADJANTONAKIS, A. K. & REINHOLDT, L. G. 2014. Derivation and characterization of mouse embryonic stem cells from permissive and nonpermissive strains. *Nat Protoc,* 9**,** 559-74.

DE SOUZA, E. J., AHMED, W., CHAN, V., BASHIR, R. & SAIF, T. 2013. Cardiac myocytes' dynamic contractile behavior differs depending on heart segment. *Biotechnol Bioeng,* 110**,** 628-36.

DIAZ-SYLVESTER, P. L., PORTA, M. & COPELLO, J. A. 2011. Modulation of cardiac ryanodine receptor channels by alkaline earth cations. *PLoS One,* 6**,** e26693.

DICK, E., RAJAMOHAN, D., RONKSLEY, J. & DENNING, C. 2010. Evaluating the utility of cardiomyocytes from human pluripotent stem cells for drug screening. *Biochem Soc Trans,* 38**,** 1037-45.

DIFRANCESCO, D. 1993. Pacemaker mechanisms in cardiac tissue. *Annual Review of Physiology,* 55**,** 455-72.

DIFRANCESCO, D. 2006. Funny channels in the control of cardiac rhythm and mode of action of selective blockers. *Pharmacol Res,* 53**,** 399-406.

DIFRANCESCO, D. 2010. The role of the funny current in pacemaker activity. *Circ Res,* 106**,** 434-46.

DIFRANCESCO, D. 2015. HCN4, Sinus Bradycardia and Atrial Fibrillation. *Arrhythm Electrophysiol Rev,* 4**,** 9-13.

DIFRANCESCO, D., DUCOURET, P. & ROBINSON, R. B. 1989. Muscarinic modulation of cardiac rate at low acetylcholine concentrations. *Science,* 243**,** 669-71.

DIFRANCESCO, D. & MANGONI, M. 1994. Modulation of single hyperpolarization-activated channels (i(f)) by cAMP in the rabbit sino-atrial node. *Journal of Physiology,* 474**,** 473-82.

DIFRANCESCO, D. & TORTORA, P. 1991. Direct activation of cardiac pacemaker channels by intracellular cyclic AMP. *Nature,* 351**,** 145-7.

ELLING, U., TAUBENSCHMID, J., WIRNSBERGER, G., O'MALLEY, R., DEMERS, S. P., VANHAELEN, Q., SHUKALYUK, A. I., SCHMAUSS, G., SCHRAMEK, D., SCHNUETGEN, F., VON MELCHNER, H., ECKER, J. R., STANFORD, W. L., ZUBER, J., STARK, A. & PENNINGER, J. M. 2011. Forward and reverse genetics through derivation of haploid mouse embryonic stem cells. *Cell Stem Cell,* 9**,** 563-74.

EROKHINA, I. L., SEMENOVA, E. G. & EMEL'IANOVA, O. I. 2005. [Human fetal ventricular cardiomyocytes in vitro: proliferation and differentiation]. *Tsitologiia,* 47**,** 200-6.

EVANS, M. J. & KAUFMAN, M. H. 1981. Establishment in culture of pluripotential cells from mouse embryos. *Nature,* 292**,** 154-6.

FASSINA, L., DI GRAZIA, A., NARO, F., MONACO, L., DE ANGELIS, M. G. & MAGENES, G. 2011. Video evaluation of the kinematics and dynamics of the beating cardiac syncytium: an alternative to the Langendorff method. *Int J Artif Organs,* 34**,** 546-58.

FRANKE, W. W., RICKELT, S., ZIMBELMANN, R., DORFLINGER, Y., KUHN, C., FREY, N., HEID, H. & ROSIN-ARBESFELD, R. 2015. Striatins as plaque molecules of zonulae adhaerentes in simple epithelia, of tessellate junctions in stratified epithelia, of cardiac composite junctions and of various size classes of lateral adherens junctions in cultures of epithelia- and carcinoma-derived cells. *Cell Tissue Res,* 359**,** 779-97.

FRIEDEL, R. H., PLUMP, A., LU, X., SPILKER, K., JOLICOEUR, C., WONG, K., VENKATESH, T. R., YARON, A., HYNES, M., CHEN, B., OKADA, A., MCCONNELL, S. K., RAYBURN, H. & TESSIER-LAVIGNE, M. 2005. Gene targeting using a promoterless gene trap vector ("targeted trapping") is an efficient method to mutate a large fraction of genes. *Proc Natl Acad Sci U S A,* 102**,** 13188-93.

FRIEDEL, R. H. & SORIANO, P. 2010. Gene trap mutagenesis in the mouse. *Methods Enzymol,* 477**,** 243-69.

FU, J. D., LI, J., TWEEDIE, D., YU, H. M., CHEN, L., WANG, R., RIORDON, D. R., BRUGH, S. A., WANG, S. Q., BOHELER, K. R. & YANG, H. T. 2006a. Crucial role of the sarcoplasmic reticulum in the developmental regulation of Ca2+ transients and contraction in cardiomyocytes derived from embryonic stem cells. *FASEB J,* 20**,** 181-3.

FU, J. D., YU, H. M., WANG, R., LIANG, J. & YANG, H. T. 2006b. Developmental regulation of intracellular calcium transients during cardiomyocyte differentiation of mouse embryonic stem cells. *Acta Pharmacol Sin,* 27**,** 901-10.

GAILLARD, S., BARTOLI, M., CASTETS, F. & MONNERON, A. 2001. Striatin, a calmodulin-dependent scaffolding protein, directly binds caveolin-1. *FEBS Lett,* 508**,** 49-52.

GARCIA-GRAS, E., LOMBARDI, R., GIOCONDO, M. J., WILLERSON, J. T., SCHNEIDER, M. D., KHOURY, D. S. & MARIAN, A. J. 2006. Suppression of canonical Wnt/beta-catenin signaling by nuclear plakoglobin recapitulates phenotype of arrhythmogenic right ventricular cardiomyopathy. *J Clin Invest,* 116**,** 2012-21.

GENTILE, A., D'ALESSANDRO, L. & MEDICO, E. 2003. Gene trapping: a multi-purpose tool for functional genomics. *Biotechnol Genet Eng Rev,* 20**,** 77-100.

GESSERT, S. & KUHL, M. 2010. The multiple phases and faces of wnt signaling during cardiac differentiation and development. *Circ Res,* 107**,** 186-99.

GHERGHICEANU, M., BARAD, L., NOVAK, A., REITER, I., ITSKOVITZ-ELDOR, J., BINAH, O. & POPESCU, L. M. 2011. Cardiomyocytes derived from human embryonic and induced pluripotent stem cells: comparative ultrastructure. *J Cell Mol Med,* 15**,** 2539-51.

GOUDREAULT, M., D'AMBROSIO, L. M., KEAN, M. J., MULLIN, M. J., LARSEN, B. G., SANCHEZ, A., CHAUDHRY, S., CHEN, G. I., SICHERI, F., NESVIZHSKII, A. I., AEBERSOLD, R., RAUGHT, B. & GINGRAS, A. C. 2009. A PP2A phosphatase high density interaction network identifies a novel striatin-interacting phosphatase and kinase complex linked to the cerebral cavernous malformation 3 (CCM3) protein. *Mol Cell Proteomics,* 8**,** 157-71.

GOURDIE, R. G., HARRIS, B. S., BOND, J., JUSTUS, C., HEWETT, K. W., O'BRIEN, T. X., THOMPSON, R. P. & SEDMERA, D. 2003. Development of the cardiac pacemaking and conduction system. *Birth Defects Res C Embryo Today,* 69**,** 46-57.

GUPTA, M. K., ILLICH, D. J., GAARZ, A., MATZKIES, M., NGUEMO, F., PFANNKUCHE, K., LIANG, H., CLASSEN, S., REPPEL, M., SCHULTZE, J. L., HESCHELER, J. & SARIC, T. 2010. Global transcriptional profiles of beating clusters derived from human induced pluripotent stem cells and embryonic stem cells are highly similar. *BMC Dev Biol,* 10**,** 98.

GUZZO, R. M., SALIH, M., MOORE, E. D. & TUANA, B. S. 2005. Molecular properties of cardiac tail-anchored membrane protein SLMAP are consistent with structural role in arrangement of excitation-contraction coupling apparatus. *Am J Physiol Heart Circ Physiol,* 288**,** H1810-9.

HALL, J., GUO, G., WRAY, J., EYRES, I., NICHOLS, J., GROTEWOLD, L., MORFOPOULOU, S., HUMPHREYS, P., MANSFIELD, W., WALKER, R., TOMLINSON, S. & SMITH, A. 2009. Oct4 and LIF/Stat3 additively induce Kruppel factors to sustain embryonic stem cell self-renewal. *Cell Stem Cell,* 5**,** 597-609.

HANNES, T., WOLFF, M., DOSS, M. X., PFANNKUCHE, K., HAUSTEIN, M., MULLER-EHMSEN, J., SACHINIDIS, A., HESCHELER, J., KHALIL, M. & HALBACH, M. 2015. Electrophysiological characteristics of embryonic stem cell-derived cardiomyocytes are cell line-dependent. *Cell Physiol Biochem,* 35**,** 305-14.

HASHEMI-TABAR, M. 2006. The effect of mouse embryonic fibroblast in direct differentiation of mouse embryonic stem cells *Iranian Journal of Reproductive Medicine,* 5.

HIROI, Y., KUDOH, S., MONZEN, K., IKEDA, Y., YAZAKI, Y., NAGAI, R. & KOMURO, I. 2001. Tbx5 associates with Nkx2-5 and synergistically promotes cardiomyocyte differentiation. *Nat Genet,* 28**,** 276-80.

HONG, Y. 2010. Medaka haploid embryonic stem cells. *Methods Cell Biol,* 100**,** 55-69.

HORIGOME, H., TAKAHASHI, M. I., ASAKA, M., SHIGEMITSU, S., KANDORI, A. & TSUKADA, K. 2000. Magnetocardiographic determination of the developmental changes in PQ, QRS and QT intervals in the foetus. *Acta Paediatr,* 89**,** 64-7.

HORII, T., MORITA, S., KIMURA, M., KOBAYASHI, R., TAMURA, D., TAKAHASHI, R. U., KIMURA, H., SUETAKE, I., OHATA, H., OKAMOTO, K., TAJIMA, S., OCHIYA, T., ABE, Y. & HATADA, I. 2013. Genome engineering of mammalian haploid embryonic stem cells using the Cas9/RNA system. *PeerJ,* 1**,** e230.

HU, N., QIAN, L. X., HU, Y., SHOU, J. Z., WANG, C. Y., GIFFEN, C., WANG, Q. H., WANG, Y., GOLDSTEIN, A. M., EMMERT-BUCK, M. & TAYLOR, P. R. 2006. Quantitative real-time RT-PCR validation of differential mRNA expression of SPARC, FADD, Fascin, COL7A1, CK4, TGM3, ECM1, PPL and EVPL in esophageal squamous cell carcinoma. *Bmc Cancer,* 6.

HUSER, J., BLATTER, L. A. & LIPSIUS, S. L. 2000. Intracellular Ca2+ release contributes to automaticity in cat atrial pacemaker cells. *J Physiol,* 524 Pt 2**,** 415-22.

HUSSAIN, W., MOENS, N., VERAITCH, F. S., HERNANDEZ, D., MASON, C. & LYE, G. J. 2013. Reproducible culture and differentiation of mouse embryonic stem cells using an automated microwell platform. *Biochem Eng J,* 77**,** 246-257.

HWANG, J. & PALLAS, D. C. 2014. STRIPAK complexes: structure, biological function, and involvement in human diseases. *Int J Biochem Cell Biol,* 47**,** 118-48.

IKONNIKOV, G., WONG, E. & CHAUDRY, S. McMaster Pathophysiology Review, www.pathophys.org

ISHII, T. M., TAKANO, M. & OHMORI, H. 2001. Determinants of activation kinetics in mammalian hyperpolarization-activated cation channels. *J Physiol,* 537**,** 93-100.

ITSKOVITZ-ELDOR, J., SCHULDINER, M., KARSENTI, D., EDEN, A., YANUKA, O., AMIT, M., SOREQ, H. & BENVENISTY, N. 2000. Differentiation of human embryonic stem cells into embryoid bodies compromising the three embryonic germ layers. *Mol Med,* 6**,** 88-95.

JAY, P. Y., HARRIS, B. S., MAGUIRE, C. T., BUERGER, A., WAKIMOTO, H., TANAKA, M., KUPERSHMIDT, S., RODEN, D. M., SCHULTHEISS, T. M., O'BRIEN, T. X., GOURDIE, R. G., BERUL, C. I. & IZUMO, S. 2004. Nkx2-5 mutation causes anatomic hypoplasia of the cardiac conduction system. *J Clin Invest,* 113**,** 1130-7.

JOUNG, B., OGAWA, M., LIN, S. F. & CHEN, P. S. 2009. The calcium and voltage clocks in sinoatrial node automaticity. *Korean Circ J,* 39**,** 217-22.

JU, Y. K. & ALLEN, D. G. 1998. Intracellular calcium and Na+-Ca2+ exchange current in isolated toad pacemaker cells. *J Physiol,* 508 (Pt 1)**,** 153-66.

KANG, J., CHEN, X. L., JI, J., LEI, Q. & RAMPE, D. 2012. Ca(2)(+) channel activators reveal differential L-type Ca(2)(+) channel pharmacology between native and stem cell-derived cardiomyocytes. *J Pharmacol Exp Ther,* 341**,** 510-7.

KAUFMAN, M. H., ROBERTSON, E. J., HANDYSIDE, A. H. & EVANS, M. J. 1983. Establishment of pluripotential cell lines from haploid mouse embryos. *J Embryol Exp Morphol,* 73**,** 249-61.

KOYANAGI, M., HAENDELER, J., BADORFF, C., BRANDES, R. P., HOFFMANN, J., PANDUR, P., ZEIHER, A. M., KUHL, M. & DIMMELER, S. 2005. Non-canonical Wnt signaling enhances differentiation of human circulating progenitor cells to cardiomyogenic cells. *J Biol Chem,* 280**,** 16838-42.

KUROSAWA, H. 2007. Methods for inducing embryoid body formation: in vitro differentiation system of embryonic stem cells. *J Biosci Bioeng,* 103**,** 389-98.

LAEMMLE, L. L., COHEN, J. B. & GLORIOSO, J. C. 2016. Constitutive Expression of GATA4 Dramatically Increases the Cardiogenic Potential of D3 Mouse Embryonic Stem Cells. *Open Biotechnol J,* 10**,** 248-257.

LAFLAMME, M. A. & MURRY, C. E. 2011. Heart regeneration. *Nature,* 473**,** 326-35.

LAHTI, A. L., KUJALA, V. J., CHAPMAN, H., KOIVISTO, A. P., PEKKANEN-MATTILA, M., KERKELA, E., HYTTINEN, J., KONTULA, K., SWAN, H., CONKLIN, B. R., YAMANAKA, S., SILVENNOINEN, O. & AALTO-SETALA, K. 2012. Model for long QT syndrome type 2 using human iPS cells demonstrates arrhythmogenic characteristics in cell culture. *Dis Model Mech,* 5**,** 220-30.

LANNER, J. T., GEORGIOU, D. K., JOSHI, A. D. & HAMILTON, S. L. 2010. Ryanodine receptors: structure, expression, molecular details, and function in calcium release. *Cold Spring Harb Perspect Biol,* 2**,** a003996.

LANT, B., YU, B., GOUDREAULT, M., HOLMYARD, D., KNIGHT, J. D., XU, P., ZHAO, L., CHIN, K., WALLACE, E., ZHEN, M., GINGRAS, A. C. & DERRY, W. B. 2015. CCM-3/STRIPAK promotes seamless tube extension through endocytic recycling. *Nat Commun,* 6**,** 6449.

LEEB, M. & WUTZ, A. 2011. Derivation of haploid embryonic stem cells from mouse embryos. *Nature,* 479**,** 131-4.

LI, J., QU, J. & NATHAN, R. D. 1997. Ionic basis of ryanodine's negative chronotropic effect on pacemaker cells isolated from the sinoatrial node. *Am J Physiol,* 273**,** H2481-9.

LIEU, D. K., LIU, J., SIU, C. W., MCNERNEY, G. P., TSE, H. F., ABU-KHALIL, A., HUSER, T. & LI, R. A. 2009. Absence of transverse tubules contributes to non-uniform Ca(2+) wavefronts in mouse and human embryonic stem cell-derived cardiomyocytes. *Stem Cells Dev,* 18**,** 1493-500.

LIU, J., DOBRZYNSKI, H., YANNI, J., BOYETT, M. R. & LEI, M. 2007. Organisation of the mouse sinoatrial node: structure and expression of HCN channels. *Cardiovasc Res,* 73**,** 729-38.

LIU, Z., LI, T., LIU, Y., JIA, Z., LI, Y., ZHANG, C., CHEN, P., MA, K., AFFARA, N. & ZHOU, C. 2009. WNT signaling promotes Nkx2.5 expression and early cardiomyogenesis via downregulation of Hdac1. *Biochim Biophys Acta,* 1793**,** 300-11.

LUDWIG, A., ZONG, X., HOFMANN, F. & BIEL, M. 1999. Structure and function of cardiac pacemaker channels. *Cell Physiol Biochem,* 9**,** 179-86.

LUNDY, S. D., ZHU, W. Z., REGNIER, M. & LAFLAMME, M. A. 2013. Structural and functional maturation of cardiomyocytes derived from human pluripotent stem cells. *Stem Cells Dev,* 22**,** 1991-2002.

LYONS, I., PARSONS, L. M., HARTLEY, L., LI, R., ANDREWS, J. E., ROBB, L. & HARVEY, R. P. 1995. Myogenic and morphogenetic defects in the heart tubes of murine embryos lacking the homeo box gene Nkx2-5. *Genes Dev,* 9**,** 1654-66.

MABLE, B. K. & OTTO, S. P. 2001. Masking and purging mutations following EMS treatment in haploid, diploid and tetraploid yeast (Saccharomyces cerevisiae). *Genet Res,* 77**,** 9-26.

MALTSEV, V. A., VINOGRADOVA, T. M. & LAKATTA, E. G. 2006. The emergence of a general theory of the initiation and strength of the heartbeat. *J Pharmacol Sci,* 100**,** 338-69.

MALTSEV, V. A., WOBUS, A. M., ROHWEDEL, J., BADER, M. & HESCHELER, J. 1994. Cardiomyocytes differentiated in vitro from embryonic stem cells developmentally express cardiac-specific genes and ionic currents. *Circ Res,* 75**,** 233-44.

MASUI, S., NAKATAKE, Y., TOYOOKA, Y., SHIMOSATO, D., YAGI, R., TAKAHASHI, K., OKOCHI, H., OKUDA, A., MATOBA, R., SHAROV, A. A., KO, M. S. & NIWA, H. 2007. Pluripotency governed by Sox2 via regulation of Oct3/4 expression in mouse embryonic stem cells. *Nat Cell Biol,* 9**,** 625-35.

MAURITZ, C., SCHWANKE, K., REPPEL, M., NEEF, S., KATSIRNTAKI, K., MAIER, L. S., NGUEMO, F., MENKE, S., HAUSTEIN, M., HESCHELER, J., HASENFUSS, G. & MARTIN, U. 2008. Generation of functional murine cardiac myocytes from induced pluripotent stem cells. *Circulation,* 118**,** 507-17.

MEURS, K. M., MAUCELI, E., LAHMERS, S., ACLAND, G. M., WHITE, S. N. & LINDBLAD-TOH, K. 2010. Genome-wide association identifies a deletion in the 3' untranslated region of striatin in a canine model of arrhythmogenic right ventricular cardiomyopathy. *Hum Genet,* 128**,** 315-24.

MEURS, K. M., STERN, J. A., SISSON, D. D., KITTLESON, M. D., CUNNINGHAM, S. M., AMES, M. K., ATKINS, C. E., DEFRANCESCO, T., HODGE, T. E., KEENE, B. W., REINA DORESTE, Y., LEUTHY, M., MOTSINGER-REIF, A. A. & TOU, S. P. 2013. Association of dilated cardiomyopathy with the striatin mutation genotype in boxer dogs. *J Vet Intern Med,* 27**,** 1437-40.

MIYAMOTO, T., FURUSAWA, C. & KANEKO, K. 2015. Pluripotency, Differentiation, and Reprogramming: A Gene Expression Dynamics Model with Epigenetic Feedback Regulation. *PLoS Comput Biol,* 11**,** e1004476.

MOLKENTIN, J. D., ANTOS, C., MERCER, B., TAIGEN, T., MIANO, J. M. & OLSON, E. N. 2000. Direct activation of a GATA6 cardiac enhancer by Nkx2.5: evidence for a reinforcing regulatory network of Nkx2.5 and GATA transcription factors in the developing heart. *Dev Biol,* 217**,** 301-9.

MORENO, C. S., LANE, W. S. & PALLAS, D. C. 2001. A mammalian homolog of yeast MOB1 is both a member and a putative substrate of striatin family-protein phosphatase 2A complexes. *J Biol Chem,* 276**,** 24253-60.

MORENO, C. S., PARK, S., NELSON, K., ASHBY, D., HUBALEK, F., LANE, W. S. & PALLAS, D. C. 2000. WD40 repeat proteins striatin and S/G(2) nuclear autoantigen are members of a novel family of calmodulin-binding proteins that associate with protein phosphatase 2A. *J Biol Chem,* 275**,** 5257-63.

MOSKOWITZ, I. P., KIM, J. B., MOORE, M. L., WOLF, C. M., PETERSON, M. A., SHENDURE, J., NOBREGA, M. A., YOKOTA, Y., BERUL, C., IZUMO, S., SEIDMAN, J. G. &

SEIDMAN, C. E. 2007. A molecular pathway including Id2, Tbx5, and Nkx2-5 required for cardiac conduction system development. *Cell,* 129**,** 1365-76.
NERBONNE, J. M. & KASS, R. S. 2005. Molecular physiology of cardiac repolarization. *Physiol Rev,* 85**,** 1205-53.
NERI, T., MERICO, V., FIORDALISO, F., SALIO, M., REBUZZINI, P., SACCHI, L., BELLAZZI, R., REDI, C. A., ZUCCOTTI, M. & GARAGNA, S. 2011. The differentiation of cardiomyocytes from mouse embryonic stem cells is altered by dioxin. *Toxicol Lett,* 202**,** 226-36.
NOBLE, D. 1979. The initiation of the heartbeat, OxfordNew York, Clarendon Press ;Oxford University Press.
OHNUKI, Y. & KUROSAWA, H. 2013. Effects of hanging drop culture conditions on embryoid body formation and neuronal cell differentiation using mouse embryonic stem cells: optimization of culture conditions for the formation of well-controlled embryoid bodies. *J Biosci Bioeng,* 115**,** 571-4.
OKADA, Y., TOTH, M. J. & VANBUREN, P. 2008. Skeletal muscle contractile protein function is preserved in human heart failure. *J Appl Physiol (1985),* 104**,** 952-7.
OTSUJI, T. G., MINAMI, I., KUROSE, Y., YAMAUCHI, K., TADA, M. & NAKATSUJI, N. 2010. Progressive maturation in contracting cardiomyocytes derived from human embryonic stem cells: Qualitative effects on electrophysiological responses to drugs. *Stem Cell Res,* 4**,** 201-13.
OXFORD, E. M., DANKO, C. G., FOX, P. R., KORNREICH, B. G. & MOISE, N. S. 2014. Change in beta-catenin localization suggests involvement of the canonical Wnt pathway in Boxer dogs with arrhythmogenic right ventricular cardiomyopathy. *J Vet Intern Med,* 28**,** 92-101.
PAL, R. 2009. Embryonic stem (ES) cell-derived cardiomyocytes: a good candidate for cell therapy applications. *Cell Biol Int,* 33**,** 325-36.
PORRELLO, E. R., MAHMOUD, A. I., SIMPSON, E., HILL, J. A., RICHARDSON, J. A., OLSON, E. N. & SADEK, H. A. 2011. Transient regenerative potential of the neonatal mouse heart. *Science,* 331**,** 1078-80.
PURVES, D. & SAKMANN, B. 1974. Membrane properties underlying spontaneous activity of denervated muscle fibres. *J Physiol,* 239**,** 125-53.
RAJALA, K., PEKKANEN-MATTILA, M. & AALTO-SETALA, K. 2011. Cardiac differentiation of pluripotent stem cells. *Stem Cells Int,* 2011**,** 383709.
RAO, J., PFEIFFER, M. J., FRANK, S., ADACHI, K., PICCINI, I., QUARANTA, R., ARAUZO-BRAVO, M., SCHWARZ, J., SCHADE, D., LEIDEL, S., SCHOLER, H. R., SEEBOHM, G. & GREBER, B. 2016. Stepwise Clearance of Repressive Roadblocks Drives Cardiac Induction in Human ESCs. *Cell Stem Cell,* 18**,** 341-53.
REBUZZINI, P., CEBRAL, E., FASSINA, L., ALBERTO REDI, C., ZUCCOTTI, M. & GARAGNA, S. 2015. Arsenic trioxide alters the differentiation of mouse embryonic stem cell into cardiomyocytes. *Sci Rep,* 5**,** 14993.
REPPEL, M., BOETTINGER, C. & HESCHELER, J. 2004. Beta-adrenergic and muscarinic modulation of human embryonic stem cell-derived cardiomyocytes. *Cell Physiol Biochem,* 14**,** 187-96.
ROBERTSON, C., TRAN, D. D. & GEORGE, S. C. 2013. Concise review: maturation phases of human pluripotent stem cell-derived cardiomyocytes. *Stem Cells,* 31**,** 829-37.
RUBENSTEIN, D. S. & LIPSIUS, S. L. 1989. Mechanisms of automaticity in subsidiary pacemakers from cat right atrium. *Circ Res,* 64**,** 648-57.
SEIFERT, R., SCHOLTEN, A., GAUSS, R., MINCHEVA, A., LICHTER, P. & KAUPP, U. B. 1999. Molecular characterization of a slowly gating human hyperpolarization-activated channel

predominantly expressed in thalamus, heart, and testis. *Proc Natl Acad Sci U S A,* 96**,** 9391-6.

SEPULVEDA, J. L., BELAGULI, N., NIGAM, V., CHEN, C. Y., NEMER, M. & SCHWARTZ, R. J. 1998. GATA-4 and Nkx-2.5 coactivate Nkx-2 DNA binding targets: role for regulating early cardiac gene expression. *Mol Cell Biol,* 18**,** 3405-15.

SHAH, M., AKAR, F. G. & TOMASELLI, G. F. 2005. Molecular basis of arrhythmias. *Circulation,* 112**,** 2517-29.

SHI, W., WYMORE, R., YU, H., WU, J., WYMORE, R. T., PAN, Z., ROBINSON, R. B., DIXON, J. E., MCKINNON, D. & COHEN, I. S. 1999. Distribution and prevalence of hyperpolarization-activated cation channel (HCN) mRNA expression in cardiac tissues. *Circ Res,* 85**,** e1-6.

SHUAI, L. & ZHOU, Q. 2014. Haploid embryonic stem cells serve as a new tool for mammalian genetic study. *Stem Cell Res Ther,* 5**,** 20.

SINGLA, D. K. & SUN, B. 2005. Transforming growth factor-beta2 enhances differentiation of cardiac myocytes from embryonic stem cells. *Biochem Biophys Res Commun,* 332**,** 135-41.

SINNECKER, D., GOEDEL, A., LAUGWITZ, K. L. & MORETTI, A. 2013. Induced pluripotent stem cell-derived cardiomyocytes: a versatile tool for arrhythmia research. *Circ Res,* 112**,** 961-8.

SINNECKER, D., MORETTI, A. & LAUGWITZ, K. L. 2014. Negating the dominant-negative allele: a new treatment paradigm for arrhythmias explored in human induced pluripotent stem cell-derived cardiomyocytes. *Eur Heart J,* 35**,** 1019-21.

SMOLICH, J. J. 1995. Ultrastructural and functional features of the developing mammalian heart: a brief overview. *Reprod Fertil Dev,* 7**,** 451-61.

SNIR, M., KEHAT, I., GEPSTEIN, A., COLEMAN, R., ITSKOVITZ-ELDOR, J., LIVNE, E. & GEPSTEIN, L. 2003. Assessment of the ultrastructural and proliferative properties of human embryonic stem cell-derived cardiomyocytes. *Am J Physiol Heart Circ Physiol,* 285**,** H2355-63.

SOTOODEHNIA, N., ISAACS, A., DE BAKKER, P. I., DORR, M., NEWTON-CHEH, C., NOLTE, I. M., VAN DER HARST, P., MULLER, M., EIJGELSHEIM, M., ALONSO, A., HICKS, A. A., PADMANABHAN, S., HAYWARD, C., SMITH, A. V., POLASEK, O., GIOVANNONE, S., FU, J., MAGNANI, J. W., MARCIANTE, K. D., PFEUFER, A., GHARIB, S. A., TEUMER, A., LI, M., BIS, J. C., RIVADENEIRA, F., ASPELUND, T., KOTTGEN, A., JOHNSON, T., RICE, K., SIE, M. P., WANG, Y. A., KLOPP, N., FUCHSBERGER, C., WILD, S. H., MATEO LEACH, I., ESTRADA, K., VOLKER, U., WRIGHT, A. F., ASSELBERGS, F. W., QU, J., CHAKRAVARTI, A., SINNER, M. F., KORS, J. A., PETERSMANN, A., HARRIS, T. B., SOLIMAN, E. Z., MUNROE, P. B., PSATY, B. M., OOSTRA, B. A., CUPPLES, L. A., PERZ, S., DE BOER, R. A., UITTERLINDEN, A. G., VOLZKE, H., SPECTOR, T. D., LIU, F. Y., BOERWINKLE, E., DOMINICZAK, A. F., ROTTER, J. I., VAN HERPEN, G., LEVY, D., WICHMANN, H. E., VAN GILST, W. H., WITTEMAN, J. C., KROEMER, H. K., KAO, W. H., HECKBERT, S. R., MEITINGER, T., HOFMAN, A., CAMPBELL, H., FOLSOM, A. R., VAN VELDHUISEN, D. J., SCHWIENBACHER, C., O'DONNELL, C. J., VOLPATO, C. B., CAULFIELD, M. J., CONNELL, J. M., LAUNER, L., LU, X., FRANKE, L., FEHRMANN, R. S., TE MEERMAN, G., GROEN, H. J., WEERSMA, R. K., VAN DEN BERG, L. H., WIJMENGA, C., OPHOFF, R. A., NAVIS, G., RUDAN, I., SNIEDER, H., WILSON, J. F., PRAMSTALLER, P. P., SISCOVICK, D. S., WANG, T. J., GUDNASON, V., VAN DUIJN, C. M., FELIX, S. B., FISHMAN, G. I., JAMSHIDI, Y., STRICKER, B. H., et al. 2010. Common variants in 22 loci are associated with QRS duration and cardiac ventricular conduction. *Nat Genet,* 42**,** 1068-76.

STERN, J. A., LAHMERS, S. & MEURS, K. M. 2015. Identification of striatin, a desmosomal protein, in the canine corneal epithelium. *Res Vet Sci,* 102**,** 182-3.

TAGLIETTI, V. & CASELLA, C. 2004. *Principi di fisiologia e biofisica della cellula,* Pavia, Goliardica pavese.

TANAKA, M., CHEN, Z., BARTUNKOVA, S., YAMASAKI, N. & IZUMO, S. 1999. The cardiac homeobox gene Csx/Nkx2.5 lies genetically upstream of multiple genes essential for heart development. *Development,* 126**,** 1269-80.

TANAKA, T., TOHYAMA, S., MURATA, M., NOMURA, F., KANEKO, T., CHEN, H., HATTORI, F., EGASHIRA, T., SEKI, T., OHNO, Y., KOSHIMIZU, U., YUASA, S., OGAWA, S., YAMANAKA, S., YASUDA, K. & FUKUDA, K. 2009. In vitro pharmacologic testing using human induced pluripotent stem cell-derived cardiomyocytes. *Biochem Biophys Res Commun,* 385**,** 497-502.

ULLOA-MONTOYA, F., VERFAILLIE, C. M. & HU, W. S. 2005. Culture systems for pluripotent stem cells. *J Biosci Bioeng,* 100**,** 12-27.

VACCARI, T., MORONI, A., ROCCHI, M., GORZA, L., BIANCHI, M. E., BELTRAME, M. & DIFRANCESCO, D. 1999. The human gene coding for HCN2, a pacemaker channel of the heart. *Biochim Biophys Acta,* 1446**,** 419-25.

VAN DER HARST, P., VAN SETTEN, J., VERWEIJ, N., VOGLER, G., FRANKE, L., MAURANO, M. T., WANG, X., MATEO LEACH, I., EIJGELSHEIM, M., SOTOODEHNIA, N., HAYWARD, C., SORICE, R., MEIRELLES, O., LYYTIKAINEN, L. P., POLASEK, O., TANAKA, T., ARKING, D. E., ULIVI, S., TROMPET, S., MULLER-NURASYID, M., SMITH, A. V., DORR, M., KERR, K. F., MAGNANI, J. W., DEL GRECO, M. F., ZHANG, W., NOLTE, I. M., SILVA, C. T., PADMANABHAN, S., TRAGANTE, V., ESKO, T., ABECASIS, G. R., ADRIAENS, M. E., ANDERSEN, K., BARNETT, P., BIS, J. C., BODMER, R., BUCKLEY, B. M., CAMPBELL, H., CANNON, M. V., CHAKRAVARTI, A., CHEN, L. Y., DELITALA, A., DEVEREUX, R. B., DOEVENDANS, P. A., DOMINICZAK, A. F., FERRUCCI, L., FORD, I., GIEGER, C., HARRIS, T. B., HAUGEN, E., HEINIG, M., HERNANDEZ, D. G., HILLEGE, H. L., HIRSCHHORN, J. N., HOFMAN, A., HUBNER, N., HWANG, S. J., IORIO, A., KAHONEN, M., KELLIS, M., KOLCIC, I., KOONER, I. K., KOONER, J. S., KORS, J. A., LAKATTA, E. G., LAGE, K., LAUNER, L. J., LEVY, D., LUNDBY, A., MACFARLANE, P. W., MAY, D., MEITINGER, T., METSPALU, A., NAPPO, S., NAITZA, S., NEPH, S., NORD, A. S., NUTILE, T., OKIN, P. M., OLSEN, J. V., OOSTRA, B. A., PENNINGER, J. M., PENNACCHIO, L. A., PERS, T. H., PERZ, S., PETERS, A., PINTO, Y. M., PFEUFER, A., PILIA, M. G., PRAMSTALLER, P. P., PRINS, B. P., RAITAKARI, O. T., RAYCHAUDHURI, S., RICE, K. M., ROSSIN, E. J., ROTTER, J. I., SCHAFER, S., SCHLESSINGER, D., SCHMIDT, C. O., et al. 2016. 52 Genetic Loci Influencing Myocardial Mass. *J Am Coll Cardiol,* 68**,** 1435-48.

VAN PETEGEM, F. 2012. Ryanodine receptors: structure and function. *J Biol Chem,* 287**,** 31624-32.

VERKERK, A. O. & WILDERS, R. 2015. Pacemaker activity of the human sinoatrial node: an update on the effects of mutations in HCN4 on the hyperpolarization-activated current. *Int J Mol Sci,* 16**,** 3071-94.

VIATCHENKO-KARPINSKI, S., FLEISCHMANN, B. K., LIU, Q., SAUER, H., GRYSHCHENKO, O., JI, G. J. & HESCHELER, J. 1999. Intracellular Ca2+ oscillations drive spontaneous contractions in cardiomyocytes during early development. *Proc Natl Acad Sci U S A,* 96**,** 8259-64.

VIDARSSON, H., HYLLNER, J. & SARTIPY, P. 2010. Differentiation of human embryonic stem cells to cardiomyocytes for in vitro and in vivo applications. *Stem Cell Rev,* 6**,** 108-20.

VINOGRADOVA, T. M., BOGDANOV, K. Y. & LAKATTA, E. G. 2002. beta-Adrenergic stimulation modulates ryanodine receptor Ca(2+) release during diastolic depolarization to accelerate pacemaker activity in rabbit sinoatrial nodal cells. *Circ Res,* 90**,** 73-9.

VINOGRADOVA, T. M., LYASHKOV, A. E., ZHU, W., RUKNUDIN, A. M., SIRENKO, S., YANG, D., DEO, S., BARLOW, M., JOHNSON, S., CAFFREY, J. L., ZHOU, Y. Y., XIAO, R. P., CHENG, H., STERN, M. D., MALTSEV, V. A. & LAKATTA, E. G. 2006. High basal protein kinase A-dependent phosphorylation drives rhythmic internal Ca2+ store oscillations and spontaneous beating of cardiac pacemaker cells. *Circ Res,* 98**,** 505-14.

WANG, K., TERRENOIRE, C., SAMPSON, K. J., IYER, V., OSTEEN, J. D., LU, J., KELLER, G., KOTTON, D. N. & KASS, R. S. 2011. Biophysical properties of slow potassium channels in human embryonic stem cell derived cardiomyocytes implicate subunit stoichiometry. *J Physiol,* 589**,** 6093-104.

WANG, X. & YANG, P. 2008. In vitro differentiation of mouse embryonic stem (mES) cells using the hanging drop method. *J Vis Exp*.

WINKLER, J., HESCHELER, J. & SACHINIDIS, A. 2005. Embryonic stem cells for basic research and potential clinical applications in cardiology. *Biochim Biophys Acta,* 1740**,** 240-8.

WOBUS, A. M. & BOHELER, K. R. 2005. Embryonic stem cells: prospects for developmental biology and cell therapy. *Physiol Rev,* 85**,** 635-78.

WOBUS, A. M., GUAN, K., YANG, H. T. & BOHELER, K. R. 2002. Embryonic stem cells as a model to study cardiac, skeletal muscle, and vascular smooth muscle cell differentiation. *Methods Mol Biol,* 185**,** 127-56.

WOODCOCK, E. A. & MATKOVICH, S. J. 2005. Cardiomyocytes structure, function and associated pathologies. *Int J Biochem Cell Biol,* 37**,** 1746-51.

XIAO, Y. F. 2003. Cardiac application of embryonic stem cells. *Sheng Li Xue Bao,* 55**,** 493-504.

YANG, H., SHI, L., WANG, B. A., LIANG, D., ZHONG, C., LIU, W., NIE, Y., LIU, J., ZHAO, J., GAO, X., LI, D., XU, G. L. & LI, J. 2012. Generation of genetically modified mice by oocyte injection of androgenetic haploid embryonic stem cells. *Cell,* 149**,** 605-17.

YI, M., HONG, N. & HONG, Y. 2009. Generation of medaka fish haploid embryonic stem cells. *Science,* 326**,** 430-3.

YING, Q. L., NICHOLS, J., CHAMBERS, I. & SMITH, A. 2003. BMP induction of Id proteins suppresses differentiation and sustains embryonic stem cell self-renewal in collaboration with STAT3. *Cell,* 115**,** 281-92.

YING, Q. L., WRAY, J., NICHOLS, J., BATLLE-MORERA, L., DOBLE, B., WOODGETT, J., COHEN, P. & SMITH, A. 2008. The ground state of embryonic stem cell self-renewal. *Nature,* 453**,** 519-23.

YOKOO, N., BABA, S., KAICHI, S., NIWA, A., MIMA, T., DOI, H., YAMANAKA, S., NAKAHATA, T. & HEIKE, T. 2009. The effects of cardioactive drugs on cardiomyocytes derived from human induced pluripotent stem cells. *Biochem Biophys Res Commun,* 387**,** 482-8.

YOUM, J. B. 2016. Electrophysiological properties and calcium handling of embryonic stem cell-derived cardiomyocytes. *Integrative Medicine Research,* 5**,** 3-10.

YU, J. & THOMSON, J. A. 2008. Pluripotent stem cell lines. *Genes Dev,* 22**,** 1987-97.

ZARAGOZA, C., GOMEZ-GUERRERO, C., MARTIN-VENTURA, J. L., BLANCO-COLIO, L., LAVIN, B., MALLAVIA, B., TARIN, C., MAS, S., ORTIZ, A. & EGIDO, J. 2011. Animal models of cardiovascular diseases. *J Biomed Biotechnol,* 2011**,** 497841.

ZHANG, J., WILSON, G. F., SOERENS, A. G., KOONCE, C. H., YU, J., PALECEK, S. P., THOMSON, J. A. & KAMP, T. J. 2009. Functional cardiomyocytes derived from human induced pluripotent stem cells. *Circ Res,* 104**,** e30-41.

ZHOU, X., QUANN, E. & GALLICANO, G. I. 2003. Differentiation of nonbeating embryonic stem cells into beating cardiomyocytes is dependent on downregulation of PKC beta and zeta in concert with upregulation of PKC epsilon. *Dev Biol,* 255**,** 407-22.